MEASUREMENT AND REDUCTION OF DYNAMICAL MECHANICAL PARAMETERS OF AQUEOUS SOLUTIONS OF MILLING YELLOW DYE

By

RICHARD ALLEN ELY

Bachelor of Science

Oklahoma State University

Stillwater, Oklahoma

1960

Submitted to the Faculty of the Graduate School of
the Oklahoma State University
in partial fulfillment of the requirements
for the degree of
MASTER OF SCIENCE
May, 1962

MEASUREMENT AND REDUCTION OF DYNAMICAL MECHANICAL PARAMETERS

OF AQUEOUS SOLUTIONS OF MILLING YELLOW DYE

Thesis Approved:

G B Thurston

Thesis Adviser

K E Harrington

Dean of the Graduate School

PREFACE

The apparatus, the mathematical relations, and the experimental techniques for the measurement of the dynamical mechanical properties of viscoelastic fluids subject to sinusoidal shear are discussed in this paper. Sample data obtained using aqueous solutions of milling yellow dye are presented. The purposes of the work were to extend previous checks of the operation of the test system and the mathematical relations, to develop a convenient means for displaying the measured dynamical mechanical properties, and to relate the measured dynamical properties to microscopic mechanisms.

The author expresses his appreciation to Dr. G. B. Thurston for many hours of patient instruction, for illuminating discussion and helpful suggestions, and for supplying and improving the test system. He expresses his appreciation also to Mr. John Schrag for aiding in the modifications of the test system, and for discussion, comments and suggestions. The author also expresses his appreciation to Mr. Heinz Hall and Mr. Frank Hargrove for their precision machining of test system components, and for their interest and cooperation. The author thanks Professor Arlo Schmidt for supplying electron microphotographs of the dye particles.

This work was made possible through Army Research Office grants for Dr. G. B. Thurston's research on the properties of viscoelastic materials. The equipment was provided by Grant Number DA-ORD-31-124-61-G58, and the general support for the work by Grant Number DA-ARO(D)-31-124-G127.

TABLE OF CONTENTS

LIST OF FIGURES

CHAPTER I

INTRODUCTION

A. Statement of the Problem

This study was undertaken in an attempt to define a technique for measuring, displaying, and describing the dynamical mechanical properties of viscoelastic fluids in sinusoidal shear at audio frequencies and below.

The fluid chosen for this study was an aqueous solution of Milling Yellow NGS, a commercial wool dye. The immediate objective was to describe, for the case of sinusoidal shear, the dependence of the real and imaginary components of the complex dynamical viscosity of the fluid upon the frequency of drive, temperature, and concentration of solute; a secondary objective was to relate the variation of the dynamical mechanical properties to the microscopic mechanisms.

On the basis of some simple assumptions regarding stress relaxations in some high polymer suspensions, Ferry[1] has developed a method whereby the simultaneous variation of the real and imaginary components of the complex dynamical viscosity with frequency, temperature, and composition can be expressed by a single empirical function for each polymer-solvent system.

An attempt was made to simplify the displaying of the results of this study by applying a method suggested by Ferry's system for reduction of variables so that the data would superpose at all temperatures,

concentrations, and frequencies of drive.

The real and imaginary components of the complex dynamical viscosity of the milling yellow solutions were obtained by applying a hydrodynamic theory developed by Thurston[2] to the measured acoustic resistance and reactance which the fluids of interest presented to a sinusoidal shear in a circular tube; Thurston[2] developed a hydrodynamic theory for the axial sinusoidal oscillation of an incompressible viscoelastic fluid in a rigid tube of infinite length and circular cross-section, using the complex coefficient of dynamical viscosity, and experimentally verified his own theory.[3]

The acoustic resistance and reactance were obtained with the aid of a hydrodynamical test system, which Thurston[4] has previously described; modifications of the system will be discussed in chapter III. The methods of other investigators apply, for audio frequencies, only to solids or very viscous fluids, and apply only at ultrasonic or subsonic frequencies for less viscous fluids.

The concepts involved in the analysis of the dynamical properties of viscoelastic substances have been outlined by Eirich[5]; the definitions and mathematical techniques have been summarized by Reiner.[6]

B. Importance of the Problem

In the past there has been no means of determining the real and imaginary components of the complex dynamical viscosity in the range of .001 to 10 poises at audio frequencies. When the real and imaginary components of the complex dynamical viscosity are both in the range of .001 to 10 poises, the shear wave length is comparable to the dimensions of commonly used test devices, so that inertial effects are large. By

using tubes, dimensions can be established which are impossible when the dimensions must apply to the acoustic source itself; thus the dimensions of the active test element can be maintained small with respect to shear wave length even in the range of .001 poise for the magnitude of the complex dynamical viscosity.

From the measurements of the dynamical properties of viscoelastic fluids of low viscosity at audio frequencies and below, a distribution of relaxation times and a molecular model may be established in the same way that they are for ultrasonic regions or for fluids of considerable viscosity. However, the low frequency, low viscosity measurements are particularly valuable for two reasons: as a rule, fewer relaxation mechanisms are excited at audio frequencies than at ultrasonic frequencies, so that a simplified study is provided which encourages and facilitates the beginning of a theory of structure. Secondly, the regions of low concentration or high temperature--in which the magnitude of the complex dynamical viscosity falls in the range of .001 to 10 poises for many substances at audio frequencies--provide a severe test of existing methods of data analysis and of existing theories of structure. It is especially valuable to observe the agreement or lack of agreement between theory and experiment in the limiting regions of the theory. Further, measurements in the region described will provide stringent checks of involved theories based on thermodynamics and statistical mechanics which have been constructed for those regions.

CHAPTER II

METHOD OF MEASUREMENT

A. The Equipment

The mechanical parameters of milling yellow were obtained from the acoustic resistance and reactance which the fluid generated during sinusoidal shear in circular brass tubes. The acoustic resistance and reactance of the tubes were measured with the aid of a hydrodynamical test system described by Thurston.[4] The acoustic signal was provided by a geophone electromagnetic driver connected to five corrugations of a Fulton Sylphon brass bellows #1002 (Sylphon catalog number 105670-27B); the Sylphon catalog lists the cross-sectional area of the bellows at 1.097 square centimeters. The geophone was driven sinusoidally from a Hewlett-Packard 202C low frequency oscillator.

The hydrodynamical test system produces three output signals: a voltage proportional to the displacement of the bellows; a voltage proportional to the velocity of the bellows; and a voltage proportional to the pressure developed across the brass tubes. All voltages were measured with a General Radio 736-A wave analyzer at 20 cycles per second and above, and with a Hewlett-Packard 403A transistor voltmeter at 20 cycles per second and below.

The construction and calibration of the hydrodynamical test system have been described by Thurston.[4] Several dimensions have been altered since Thurston's description, so that the values of the

sensitivities and system residuals have been modified. Figure 1 shows some of the basic elements of the hydrodynamical test system and temperature controlling water bath--explained below--, and gives the present dimensions.

The present volume flow sensitivity is 1.522 cubic centimeters per second per volt out of the velocity monitor. The coils in the velocity monitor have been wound on lucite coil forms in order to avoid eddy currents and phase errors.

The pressure sensitivity varies a few per cent from day to day from 3.40×10^4 dynes per square centimeter per volt of output from the pressure monitor. The pressure is no longer sensed by means of a capacity hydrophone utilizing Sylphon bellows, as in earlier descriptions[4]; Thurston obtained a more desirable shunt impedance by replacing the pressure-sensing bellows with a capacitive microphone of his own design. The pressure sensitivity is no longer obtained by means of a hydrostatic head as previously described,[4] but by means of a brass tube of known impedance.

An electronic summing circuit is utilized to determine the component of pressure in phase with the volume velocity and the component of pressure in phase quadrature with the volume velocity--in phase with the displacement. If the in-phase component is denoted by ρ_c, and the out-of-phase component is denoted by ρ_s, the pressure ρ may be written as

$$\rho = \rho_c \cos \omega t + \rho_s \sin \omega t, \qquad (2.1)$$

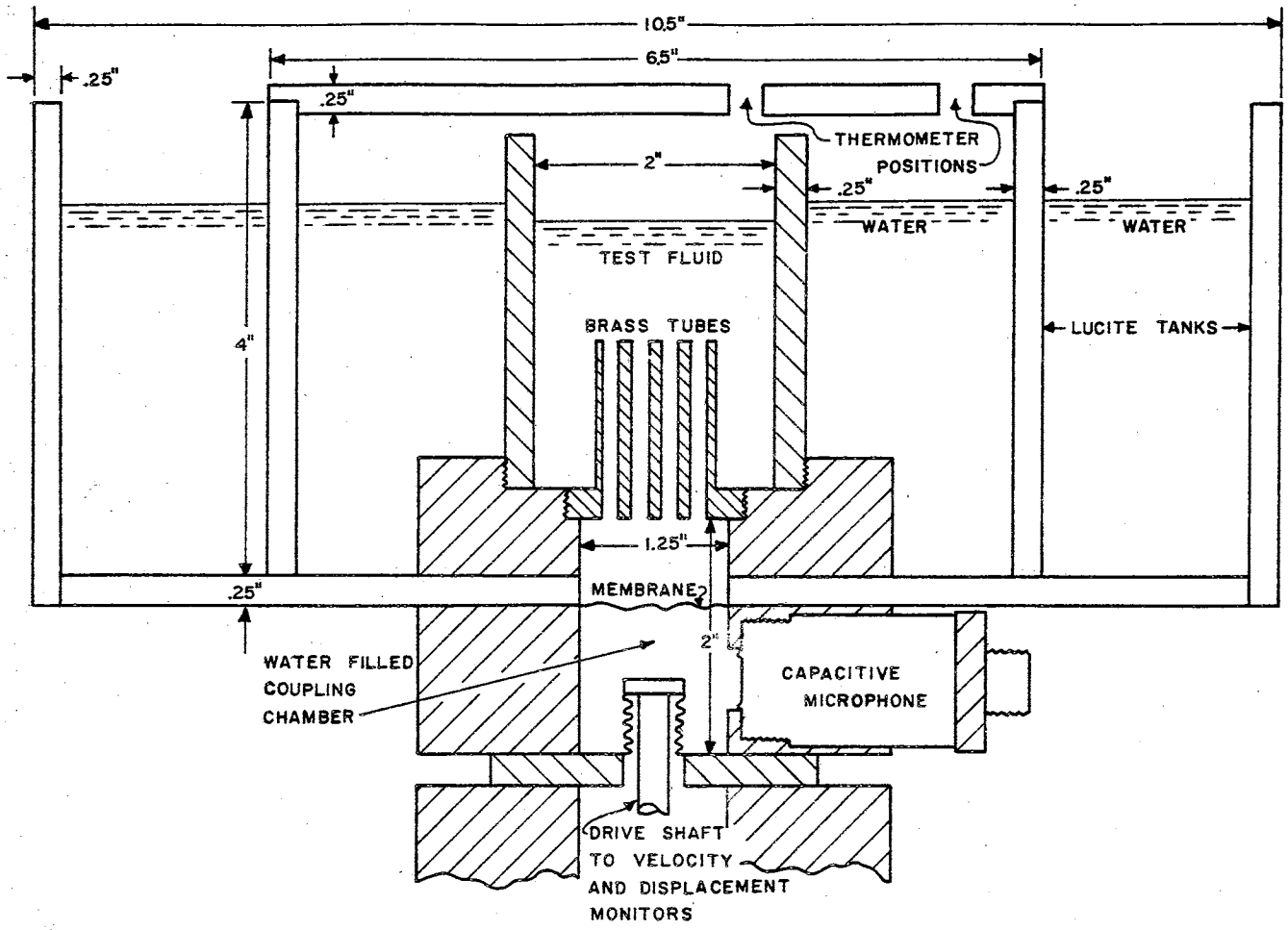

Figure 1. A simplified drawing of the hydrodynamical test system and temperature controlling water bath.

where ω is the angular frequency and t is time; then the measured acoustic resistance is

$$R = p_c / u_m , \tag{2.2}$$

where u_m is the magnitude of the volume velocity, and the measured acoustic reactance is

$$X = p_s / u_m . \tag{2.3}$$

A block diagram of all the test equipment is displayed in figure 2. Figure 3 is a photograph of all equipment used, while figure 4 is a photograph of the hydrodynamical test system and temperature controlling water bath.

The impedance of the brass tubes must be corrected for the presence of the impedance of the chamber coupling tubes and driver. The correction is accomplished in a manner analagous to the treatment of standard alternating current circuits. Figure 5 illustrates the schematic circuit for the acoustic elements of the system. The shunt compliance and resistance of the coupling chamber were measured by sealing the chamber with a 1/8 inch brass plate while using water as the test fluid. Previous measurements[3] made by sealing the tubes with a weight had indicated that the shunt impedance varied with changing test fluid, but later checks indicated that variable sealing was being established and the leakage impedance, not the shunt impedance, was a function of changing test fluid. The value established for the shunt compliance was 8.72×10^{-9} gram^{-1} centimeter^4. The resistance

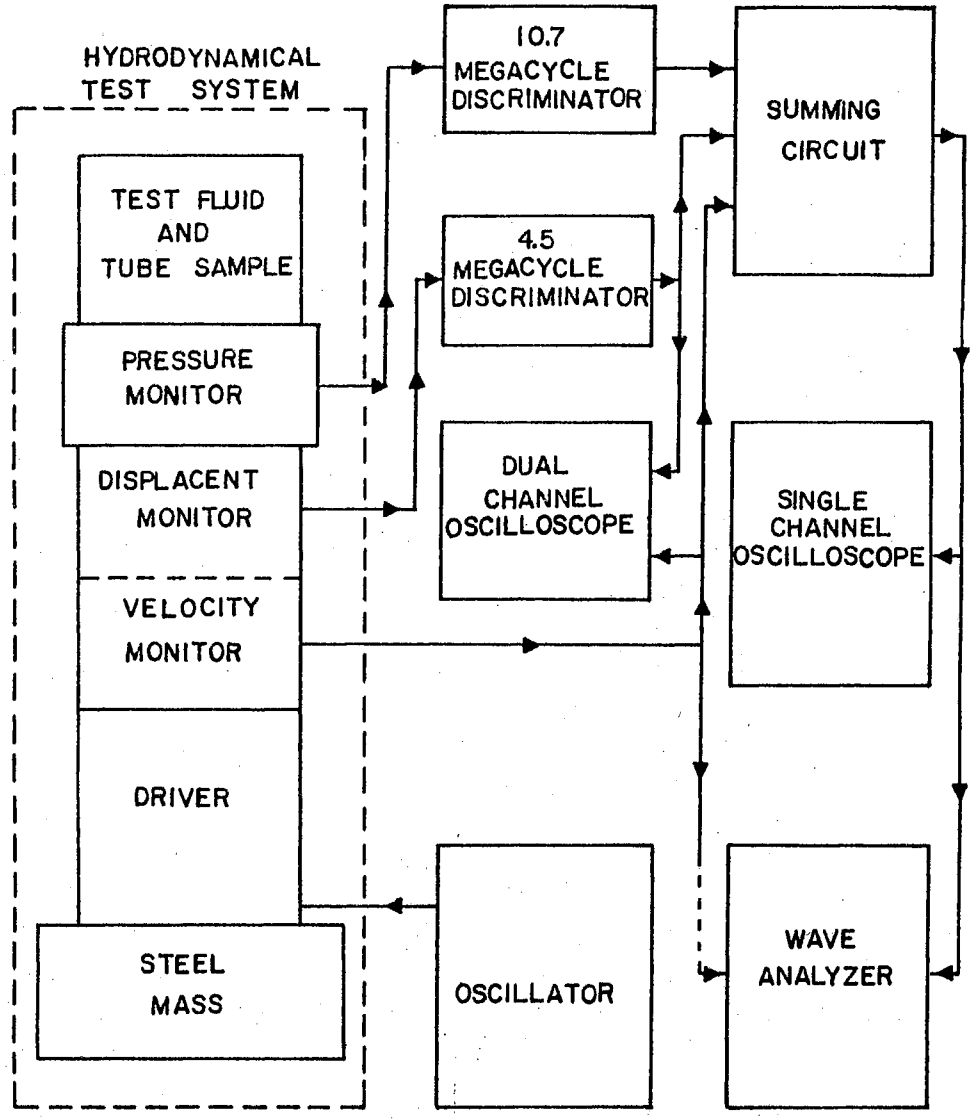

Figure 2. A block diagram of the hydrodynamical test system and associated electronic equipment.

FIGURE LEGEND

Figure 3. A photograph of the hydrodynamical test system and associated electronic equipment

A. The hydrodynamical test system and temperature controlling water bath
B. 4.7 megacycle displacement discriminator
C. Vacuum tube voltmeter (RCA Senior Voltohmyst)
D. Heathkit PS-3 power supply
E. Hewlett-Packard 522B frequency counter
F. General Radio 736A wave analyzer
G. DuMont 322A dual beam oscilloscope
H. DuMont 304A single beam oscilloscope
I. Hewlett-Packard 202C audio oscillator
J. 10.7 megacycle pressure discriminator
K. Summing circuit

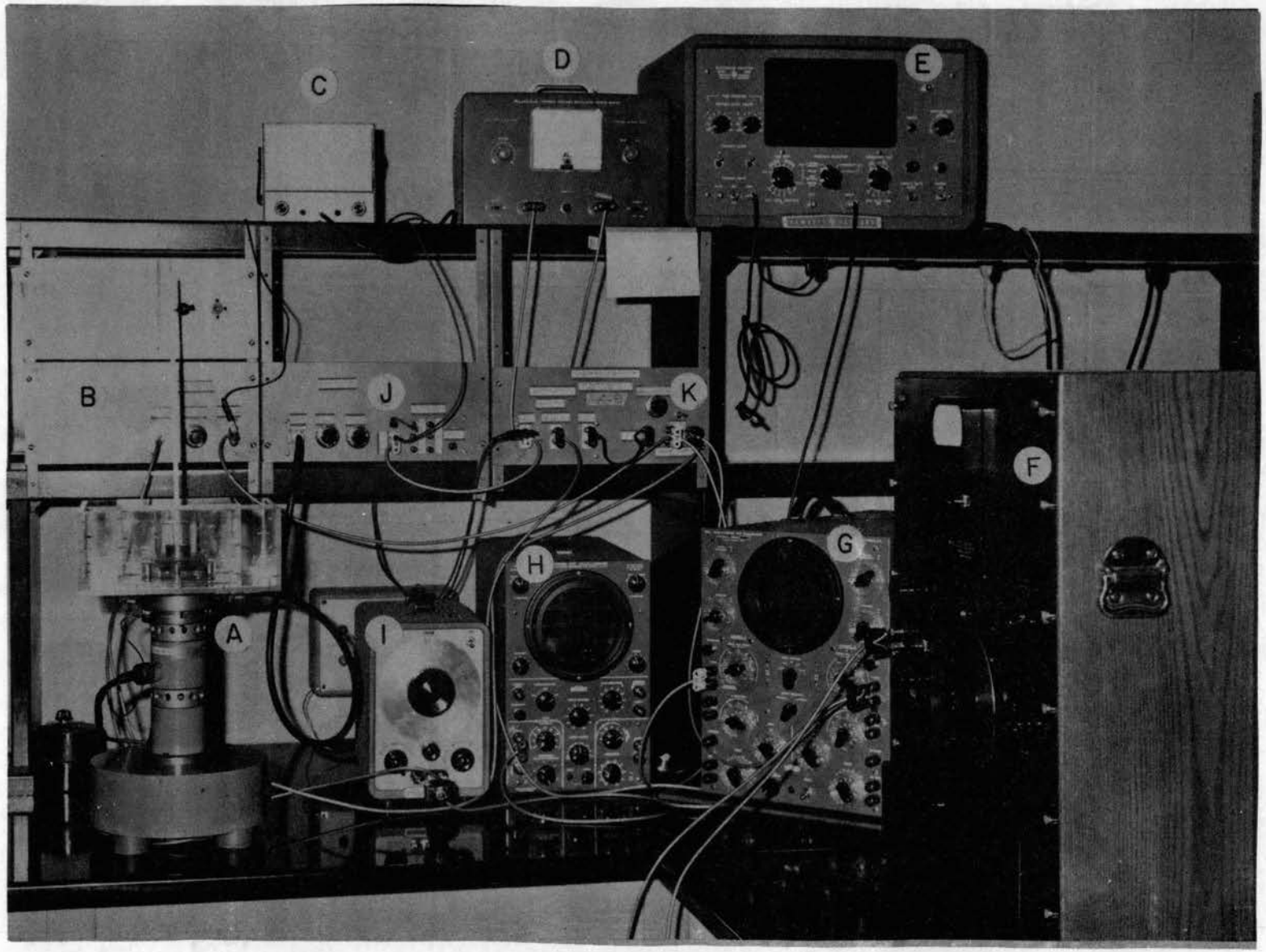
A
B
C
D
E
F
G
H
I
J
K

FIGURE LEGEND

Figure 4. A photograph of the hydrodynamical test system and temperature controlling water bath

A. Thermometers--one in test fluid, one in inner bath
B. Test fluid
C. Tube sample
D. Pressure sensing chamber
E. Capacitive microphone
F. Moving coil velocity monitor
G. Moving coil driver
H. Steel block
I. Rubber stoppers

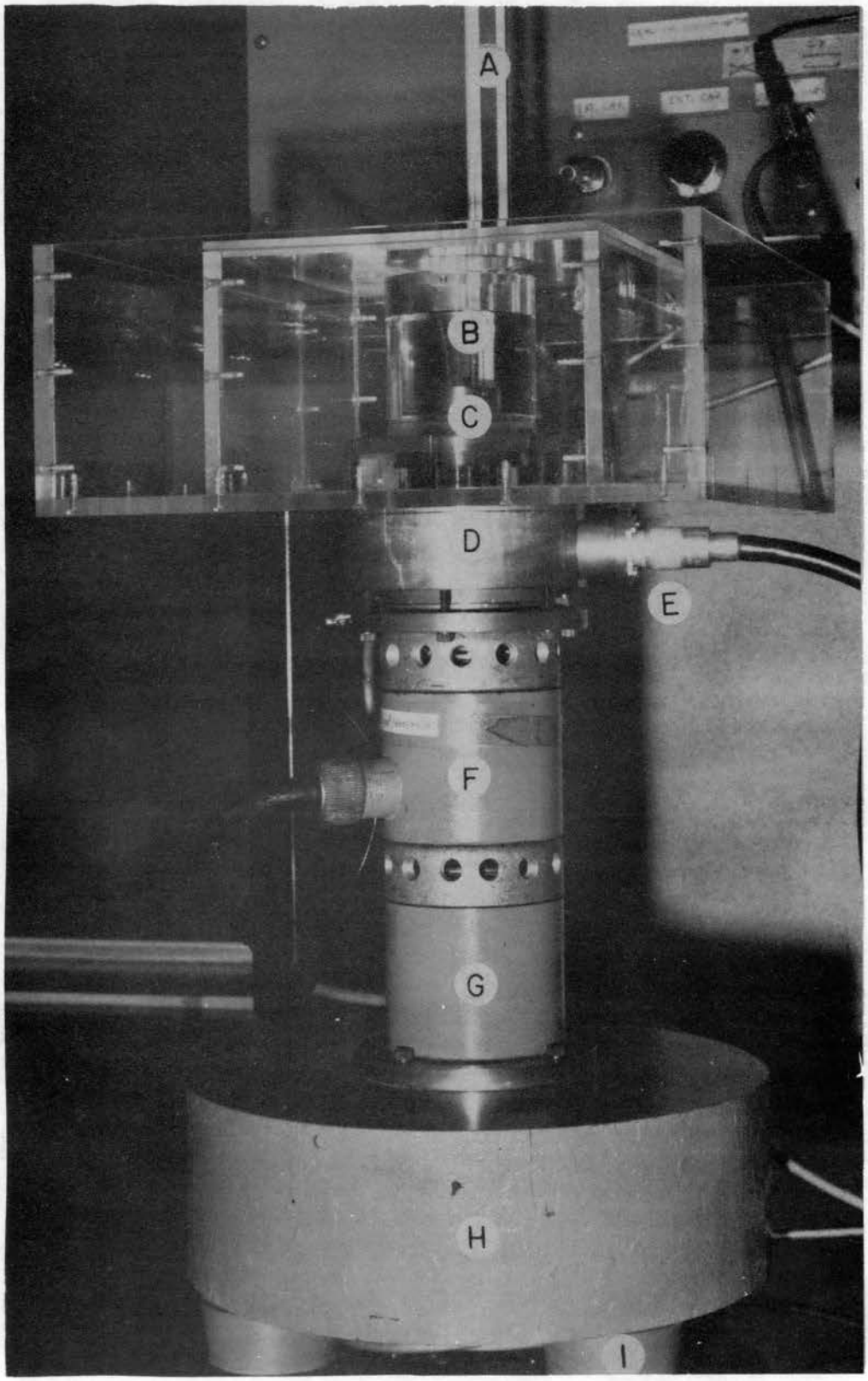
A
B
C
D
E
F
G
H
I

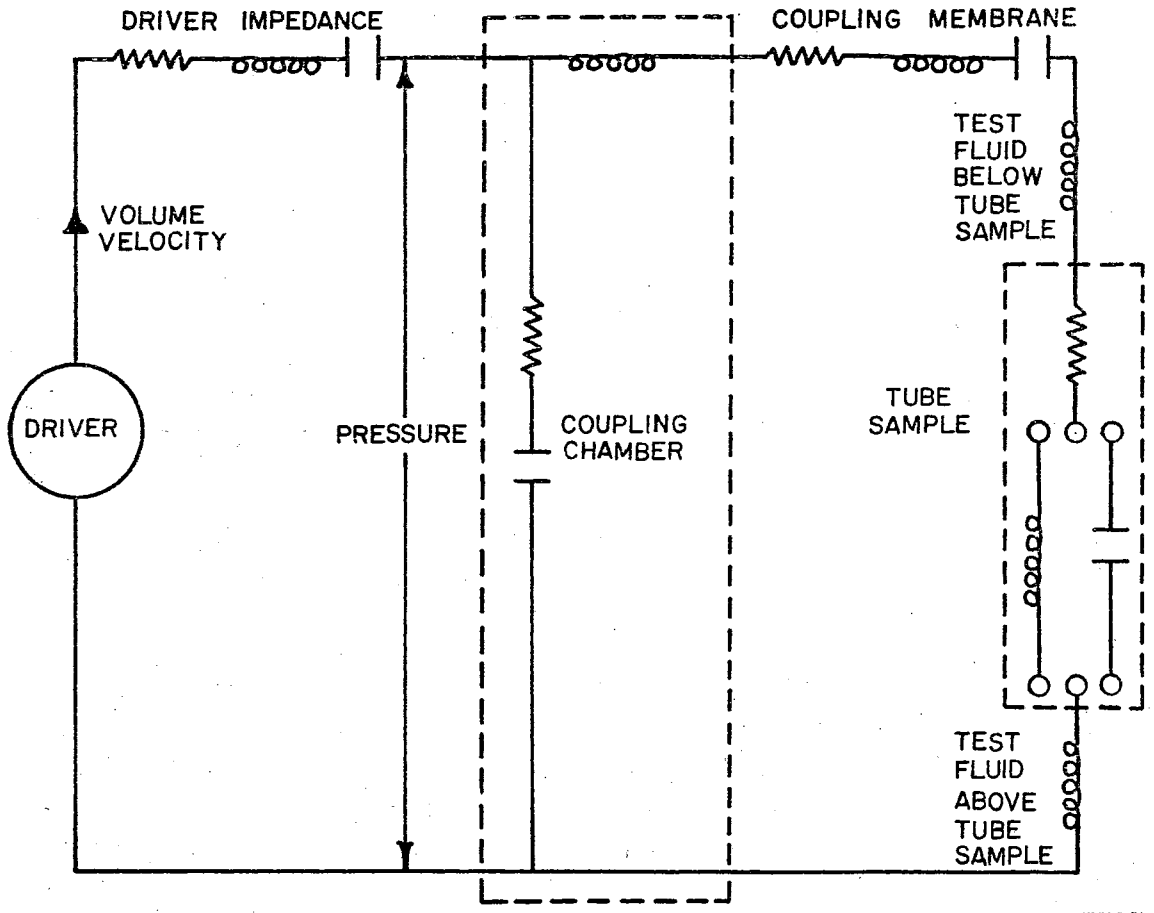

Figure 5. A schematic circuit for the acoustic elements of the hydrodynamical test system.

varied with changing frequency, and ranged from 1.75×10^5 gram centimeter^{-4} second^{-1} at 20 cycles per second to 9.00×10^3 gram centimeter^{-4} second^{-1} at 200 cycles per second. The inertance of the coupling chamber and the inertance of the test fluid above and below the brass tube combine to yield an inertance of .558 gram centimeter^{-4} if there is one inch of test fluid above the sample; one component of this series inertance will vary in direct proportion to the variation of the density of the water in the lower chamber, and one component will vary in direct proportion to the variation of the density of the test fluid. The series compliance of the polyethylene membrane separating the lower chamber from the test chamber is 5.58×10^{-5} gram^{-1} centimeter^4 at 50 cycles per second and 24 degrees centigrade, and the series inertance of the membrane is .217 gram centimeter^{-4} units at 50 cycles per second and 24 degrees centigrade.

Temperature control was achieved by means of a non-circulating water bath which was contained by a double walled lucite box; the dimensions of the lucite box are given in figure 1. The portion of the bath surrounding the sample holder and test fluid was provided with a close fitting lucite cover. Thermometers were placed through holes in the lid into the test fluid and water bath.

In preliminary measurements the fluid was first established at a temperature removed from room temperature and the mechanical properties observed while the fluid returned to room temperature; then the fluid was established at room temperature and the mechanical properties observed while the fluid moved away from room temperature--no significant differences in the mechanical properties of the fluid at a given temperature were noted for the two cases. Any error in the measurement

of the temperature probably would have manifested itself as an inconsistency at this point. Measurements of the mechanical properties of the fluid versus temperature were conducted using brass components and using lucite for all components except the tubes; no significant differences in the mechanical properties of the fluid at a given temperature were noted for the two cases; again there must have been no serious errors in the measurement of the temperature of the test fluid. However, use of brass components facilitated the experiment, since it hastened the temperature changes. It was necessary to establish the bath at 80 degrees centigrade several times in order to raise the test fluid to 70 degrees centigrade. Ice water was placed in the bath in order to lower the temperature--it required about one-half hour to cool the test fluid to three degrees centigrade if the brass components were used.

The sensing elements of the hydrodynamical test system were isolated from the test fluid and sample holder by the 1/4 inch lucite container which held the water bath and by the polyethylene membrane which separated the test fluid from the lower chamber; feeling the portion of the hydrodynamical test system containing the sensing elements indicated that it did not deviate seriously from room temperature after maintaining the test fluid about 20 centigrade degrees below room temperature or about 40 centigrade degrees above room temperature for many hours.

Measurements indicate that the shunt impedance does not vary significantly with temperature. Possible temperature variations of the impedance of the polyethylene membrane were not investigated, since the correction for the membrane impedance is small.

B. Range of the Measured Parameters

The measured sample impedances must not be allowed to far exceed 1/10th of the value of the shunt impedance at a given frequency, or the corrections are undesirably large. Inertial forces must not be allowed to become comparable to viscous and elastic forces if accurate measurements and calculations are to result. These two restrictions provide limits on tube diameter, tube length, number of tubes per sample, magnitude of the complex dynamical viscosity of the test fluid, and frequency. The tube samples available allow the restrictions to be satisfied if the magnitude of the complex dynamical viscosity ranges from .01 poise to 10 poises while the components of the complex dynamical viscosity vary from .001 poise to 10 poises and the frequency ranges from 2 cycles per second to 200 cycles per second if proper tube interchanges are conducted at crucial points. Ratios of sample impedances for a fluid in question to sample impedances of a known fluid allow estimates of the magnitude of the complex dynamical viscosity sufficient for assigning samples.

Volume velocities must be experimentally determined for each combination of fluid, tube, and frequency in order to avoid nonlinearity. The volume velocity is adjusted so that halving or doubling the volume velocity results in halving or doubling the pressure across the tubes.

The tube samples available range from 55 tubes at .03 centimeter diameter to 4 tubes at .7 centimeter diameter. Samples with more tubes would extend the range of measureable components of the complex dynamical viscosity.

C. Determination of the Real and Imaginary Components of the Complex Dynamical Viscosity from Primary Data

Thurston[2] has obtained expressions for the acoustic resistance and reactance of a homogeneous, isotropic viscoelastic fluid for the case of sinusoidal shear in a circular tube. The expressions are valid for restricted values of a dimensionless parameter (Ka) defined by

$$(Ka)=a\sqrt{\rho w/\eta}\,, \tag{2.4}$$

where ρ is the fluid density,

w is the angular frequency,

a is the tube radius,

and η is the magnitude of the complex dynamical viscosity.

(Ka) can be interpreted as an indicator of the significance of inertial forces. For most purposes (Ka) must remain smaller than 1. The expression for the imaginary part of the complex dynamical viscosity is not valid in the region of viscoelastic resonance; viscoelastic resonance occurs when

$$(Ka)=\sqrt{6\sin\phi}\,, \tag{2.5}$$

where ϕ is related to the complex dynamical viscosity, η^*, by

$$\eta^*=\eta'-i\eta''=\eta e^{-i\phi}, \tag{2.6}$$

where η is the magnitude of the complex dynamical viscosity.

When the expressions for the acoustic resistance and reactance of the fluid are solved for the components of the complex dynamical viscosity the result is

$$\eta' = \frac{\rho\omega a^2}{8} P_0 \tag{2.7}$$

$$\eta'' = \frac{\rho\omega a^2}{8}\left(\frac{4}{3} - Q_0\right), \tag{2.8}$$

where P_0 is the value of P for (Ka) small,

and Q_0 is the value of Q for (Ka) small;

P and Q are defined by

$$P = \frac{RN}{\rho\omega l_e/\pi a^2} \tag{2.9}$$

$$Q = \frac{XN}{\rho\omega l_e/\pi a^2}, \tag{2.10}$$

where N is the number of tubes in the brass sample,

R is the measured acoustic resistance of the sample,

X is the measured acoustic reactance of the sample,

and l_e is an effective length[7] given by

$$l_e = l + 1.698a, \tag{2.11}$$

where l is the actual tube length.

The calculations of η' and η'' were carried through with the aid of an IBM 650 digital computer, since the calculations involved in correcting for shunt impedance are time consuming.

The measured parameters P and Q provide a check of the theory which yielded equations (2.7) and (2.8), since that theory requires that P and Q be given respectively by the real and imaginary parts of the function

$$\left[\frac{2i}{k^*a}\,\frac{J_1(k^*a)}{J_0(k^*a)} - i\right]^{-1}, \tag{2.12}$$

where J_0 and J_1 are zero and first order Bessel functions, and

$$k^* = \left[i\rho\omega/\eta^*\right]^{1/2}. \tag{2.13}$$

Curves for P and Q versus (ka) have been prepared[3] from measurements of acoustic resistance and reactance for several substances including aqueous milling yellow solutions and distilled water, and for many tube diameters, and good agreement with theory was obtained.

D. The Test Fluid

Milling yellow is one of a group of dyes known as yellow mordant azo dyes.[8] Milling yellow is used in wool dying, and, being a mordant dye, in color photography.

The milling yellow used for this study was Milling Yellow NGS, a product of National Aniline Division. It is obtained in the form of a dry, yellow, finely divided solid. Private correspondence[9] revealed that the chemical structure for Milling Yellow NGS is

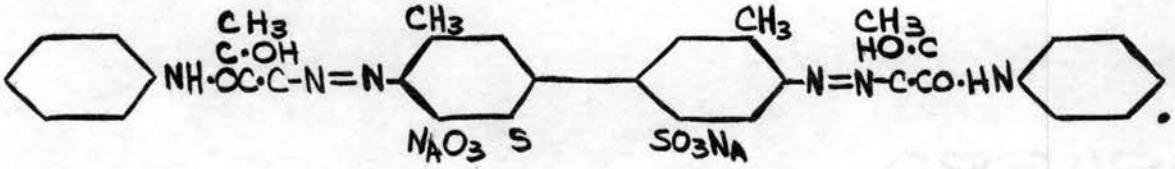

Freundlich and Gillings[10] recorded the optical and mechanical properties of a substance physically similar to Milling Yellow NGS, and, with the aid of an optical microscope, observed rod-shaped particles in aqueous solutions. They used a substance they called cotton yellow, which was British Company's "Chlorazol Fast Yellow 5GKS"; the structural formula for that substance is[10]

The dry milling yellow is not significantly soluble in water at room temperature, but is readily soluble in boiling water. The solutions used in this study were prepared by two methods. The first method consisted of adding the proper amount of milling yellow to boiling distilled water, boiling gently for twenty minutes, filtering immediately, and setting the fluid aside to allow it to cool to room temperature undisturbed. The second method consisted of diluting a fluid of known concentration with distilled water, reboiling momentarily and refiltering. The fluids were filtered to remove impurities which sometimes serve as

nuclei of crystallization. During the boiling process the bottom of the container must not be heated too quickly or the fluid is "scorched" and discolors.

ELectron microphotographs indicate that the "raw" milling yellow and milling yellow obtained by drying a prepared solution are composed of ellipsoidal particles whose dimensions vary widely but average about 2×10^{-4} centimeter long and 6×10^{-5} centimeter in diameter; these dimensions agree with dimensions obtained by Prados and Peebles[11] from optical measurements on aqueous milling yellow solutions. There is some question as to whether the particles maintain their identity in solution regardless of temperature or concentration. The previously mentioned observations of Freundlich and Gillings[10] of rod-shaped particles in aqueous solutions similar to Milling Yellow NGS solutions might cause one to suspect that the particles do maintain their rigid ellipsoidal form in solution. Further, microscopic examinations of the Milling Yellow NGS aqueous solutions were included in the study being presented, and rod-shaped particles could be seen whose size agreed with the electron microphotographs. However, the reproducibility of the microscopic observation of the rod-shaped particles was so poor that one must consider the possibility that the particles were produced by non-reproducible surface effects. Further evidence that there are rigid ellipsoidal particles in the aqueous milling yellow solutions will be presented in chapter V, and evidence that the particles do not maintain their identity with changing concentration and temperature will be presented in chapter IV.

The concentrations of the aqueous milling yellow solutions were determined by two methods. The first method consisted of taking the

ratio of the weight of milling yellow added to the water and the weight of the final solution. The second method consisted of placing a known weight of solution in a 10 cubic centimeter bottle and heating at 90 degrees centigrade for at least 12 hours after the solvent was evaporated--the concentration was then the weight of the residue divided by the weight of the original solution. Both methods were sufficiently accurate for this study, but the first method should not be expected to yield errors smaller than one per cent, for the dry milling yellow is hygroscopic--its weight will vary with humidity and time exposed to open air. Since the milling yellow is hygroscopic, great care must be exercised to cause even the second method to yield errors smaller than one per cent. The weighing bottle should be provided with a stopper so that the "dry" air resulting from heating may be trapped above the residue before the bottle and residue are weighed. It should not be necessary to use stop-cock grease at 90 degrees centigrade; if stop-cock grease is used, the greased stopper should be included in the heating process to drive out trapped moisture. In any case, the heating and weighing process should be carried out in the same way for the empty bottle as for the bottle containing the dry residue, except that one hour heating time suffices for the empty bottle. Unless precautions are taken, or equilibrium conditions at constant humidity are established, the condensation of water vapor on the outside of the hot, stoppered bottle during the weighing process will generate error.

Aqueous milling yellow solutions were chosen for this study because they are strongly viscoelastic at concentrations in the range of 1 to 2 per cent by weight. The solutions are also brilliantly birefringent at concentrations in the range of 1.4 to 2 per cent by weight at room

temperature, so that they provide an excellent opportunity for relating optical phenomena with mechanical phenomena. Further, milling yellow is inexpensive, readily available, and the solutions are not difficult to prepare and handle, and do not have offensive odors.

If the aqueous milling yellow solutions are prepared in carefully cleaned containers and are protected from air-borne debris, they are stable for many months.

Measurements of the acoustic resistance and reactance of lucite tubes and brass tubes of identical dimensions under identical test conditions indicate no dependence of the mechanical properties of the fluid on tube material.

Steady flow measurements of the optical properties of aqueous milling yellow solutions have been conducted by Prados and Peebles[11]; steady flow measurements of the mechanical properties of aqueous milling yellow solutions have been conducted by Honeycutt and Peebles.[12]

CHAPTER III

REDUCTION OF PARAMETERS

A. Introduction

Measurements of the mechanical properties of fluids are difficult to interpret and extrapolate when referred to literal molecular models. For some classes of fluids under proper measurement conditions the use of mechanical models analagous to the actual molecular mechanisms has made it possible to predict the results of measurements of the mechanical properties of fluids without explicit descriptions of the statistical mechanics, thermodynamics, and hydrodynamics of the fluid.[13,14,15,16] Since analagous mechanical models make it possible to combine many parameters, the analogs obviate the need for writing explicit equations for the temperature, frequency, and concentration dependence of the mechanical parameters of fluids; such equations are usually very difficult to write over any useful range of parameters, since the mechanical parameters of the fluid vary in too complicated a manner.

Some investigators have, with little or no theoretical justification,[17] combined data at different frequencies and temperatures by shifting the coordinates of the curves displaying the logarithm of the real and imaginary parts of the complex dynamical viscosity versus the logarithm of the frequency. The use of analagous mechanical models leads to a reduced parameter theory which justifies the coordinate shifts.

B. The Maxwell Specification of Fluids

The Maxwell specification of fluids[18] states that the behavior of an isotropic viscoelastic fluid in small deformations corresponds to the behavior of a parallel array of Maxwell elements,[19] providing that the fluid obeys the superposition principle.[20] The parallel array is shown in figure 8 and will be discussed after the individual elements are described.

The Maxwell element consists of a spring which has a rigidity of G_∞ in series with a dashpot which has a viscosity of η_o , as shown in figure 6.

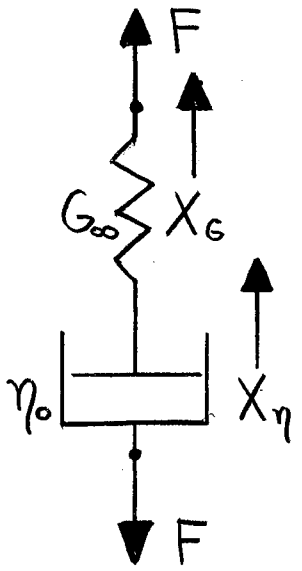

Figure 6. A Maxwell element consisting of a spring of rigidity G_∞ in series with a dashpot of viscosity η_o . A force F acts across the spring and dashpot, causing a displacement X_G across the spring and a displacement X_η across the dashpot.

The spring is Hookian--the force across the spring is proportional to the extension. The dashpot is Newtonian--the rate of extension is proportional to the force across the dashpot. The force exerted across the model is

common to the spring and dashpot. If the model is acted on by a force F, as shown in figure 6, the displacement of the spring, X_G, will be given by Hooke's law

$$F = G_\infty X_G, \tag{3.1}$$

and the displacement of the dashpot, X_η, will be given by Newton's law

$$F = \eta_0 \dot{X}_\eta, \tag{3.2}$$

where $\dot{X}_\eta$ is the time derivative of X_η. The total displacement, X, is the sum of the displacements of the spring and dashpot; then

$$X = X_G + X_\eta. \tag{3.3}$$

If the spring and dashpot connect two unit areas a unit length apart, the force F is analagous to the shearing stress T acting on a unit dimension cube of the fluid to be described, and the displacement X of the spring and dashpot combination is the same as the extension e of the cube of test material. Under these conditions the spring and dashpot can represent a unit volume of the fluid to be described (if the fluid exhibits only one relaxation mechanism). Figure 7 shows a unit dimension cube of the fluid to be described by a Maxwell element. The fluid is acted on by a shearing stress T and consequently undergoes an extension e.

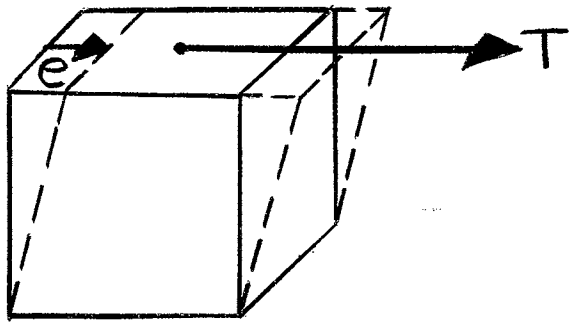

Figure 7. A unit dimension cube of the fluid to be described by a Maxwell element. The fluid is acted upon by a shearing stress T and consequently undergoes an extension e.

If equations (3.1) and (3.2) are rewritten in terms of the shearing stress and the strain (for the case described by figure 7) the result is

$$T = G_\infty e_G \tag{3.4}$$

$$T = \eta_0 \dot{e}_\eta, \tag{3.5}$$

where e_G is the strain exhibited by the spring, and $\dot{e}_\eta$ is the time derivative of e_η --the strain exhibited by the dashpot. If equation (3.4) is solved for the time rate of extension and added to the rate of extension given by equation (3.5) the result is

$$\dot{e} = \frac{T}{\eta_0} + \frac{\dot{T}}{G_\infty}, \tag{3.6}$$

where $\dot{e}$ is the time rate of extension of the unit cube of material,

and $\dot{T}$ is the time rate of shearing stress.

The rate of extension may be rewritten for sinusoidal deformation by introducing a complex dynamical shear viscosity which has been justified by thermodynamic considerations[21] and by analogy with alternating current circuit theory.[22] The complex shear viscosity, η^*, is defined as

$$\eta^* = \eta' - i\eta'' = \frac{T}{\dot{e}}. \tag{3.7}$$

Introducing equation (3.7) into equation (3.6) yields

$$\dot{e} = \frac{T}{\eta^*} = \frac{T}{\eta_0} + \frac{\dot{T}}{G_\infty}. \tag{3.8}$$

For sinusoidal processes T may be represented by

$$T = T_{max} e^{i(\omega t + \delta)}, \tag{3.9}$$

where t is time, ω is the angular frequency, δ is some phase angle, and T_{max} is the maximum value of T ; then

$$\dot{T} = i\omega T. \tag{3.10}$$

Substituting equation (3.10) in equation (3.8) and dividing by T yields

$$\frac{1}{\eta^*} = \frac{1}{\eta_0} + i\frac{\omega}{G_\infty}. \tag{3.11}$$

Solving equation (3.11) explicitely for η^* one obtains

$$\eta^* = \frac{1}{\frac{1}{\eta_0} + i\frac{\omega}{G_\infty}} = \frac{\eta_0 G_\infty}{G_\infty + i\eta_0\omega} = \frac{\eta_0 G_\infty (G_\infty - i\eta_0\omega)}{G_\infty^2 + \eta_0^2\omega^2} . \tag{3.12}$$

If $\frac{\eta_0}{G_\infty}$ is defined as the ralaxation time J , equations (3.7) and (3.12) yield

$$\eta' = \frac{\eta_0 G_\infty^2}{G_\infty^2 + \eta_0^2\omega^2} = \frac{\eta_0}{1 + \left(\frac{\eta_0}{G_\infty}\right)^2\omega^2} = \frac{G_\infty J}{1 + J^2\omega^2} . \tag{3.13}$$

$$\eta'' = \frac{\eta_0^2 G_\infty \omega}{G_\infty^2 + \eta_0^2\omega^2} = \frac{G_\infty \omega}{\left(\frac{G_\infty}{\eta_0}\right)^2 + \omega^2} = \frac{G_\infty \omega J^2}{1 + J^2\omega^2} \tag{3.14}$$

$$\eta_s = G_\infty J, \tag{3.15}$$

where η_s is the value of η' for $\omega J \ll 1$; if the deformations are large, η_s becomes what is often referred to as the steady flow viscosity. The magnitude of the complex dynamic viscosity is given by

$$\eta = (\eta'^2 + \eta''^2)^{1/2} . \tag{3.16}$$

Substitution of equations (3.13) and (3.14) into equation (3.16) yields

$$\eta^2 = \frac{G_\infty^2\omega^2 J^4 G_\infty^2 J^2}{(1 + \omega^2 J^2)^2} = \frac{G_\infty^2 J^2 (1 + \omega^2 J^2)}{(1 + \omega^2 J^2)^2} = \frac{G_\infty^2 J^2}{1 + \omega^2 J^2}, \tag{3.17}$$

or $$\eta = \frac{G_\infty J}{(1 + \omega^2 J^2)^{1/2}} . \tag{3.18}$$

Alfrey[19] states that the Maxwell specification is founded on the

following visualization of actual molecular phenomena: "The stress on a given cross section of the material is supported by interatomic or intermolecular forces exerted upon the atoms and molecules lying in the cross section. These forces may be given the generic name of 'bonds' connecting the material on the two sides of the cross section. Each of these bonds will have its own stiffness and its own characteristic rate of relaxation. A distribution of elastic relaxation times is thus correlated on the molecular scale with a distribution in the relaxation times of the interparticle bonds."

Gemant[22] noticed that equation (3.6) may be compared to a similar equation for electric current, where the current is composed of two terms: one in phase with voltage T --corresponding to the current in a resistance η_0 --, and the other in phase quadrature--corresponding to a current in a capacitance $1/G_\infty$. η^* in equation (3.8) can be compared to the complex electrical impedance established by a resistance η_0 and a capacitive reactance G_∞/W. In this electromechanical analogy of the first kind[23]--the impedance analogy-- in which electromotive force is analagous to mechanical force, electric current to velocity, mass to inductance, compliance to capacitance, and mechanical resistance to electrical resistance, the electrical analog of the mechanical parallel circuit is the electrical series circuit. The reason for the difference in structure between the two circuits is that voltage is common to all the elements in a parallel electric circuit, while force--analogous to voltage--is additive in a parallel mechanical circuit; further, the current is additive in a parallel electrical circuit, while rate of extension--analogous to current--is common to all the elements in a parallel mechanical circuit.

The impedance analogy justifies the conclusion of Ferry, Sawyer, and Ashworth[13]: "The equations for frequency dependence of G', η', and $|G|$ for any model can be obtained by strict analogy with the treatment of alternating current circuits, adding the components of G (or η) when they appear in parallel and adding their reciprocals when they appear in series."

According to the Maxwell specification[19] of fluids referred to earlier, more complex fluids may be represented by an unlimited number of Maxwell elements in parallel and with a continuous distribution of relaxation times.[24] Figure 8 presents the parallel assemblage of Maxwell elements representing the unit cube of the complex fluid subjected to a shearing stress T and undergoing an extension e. The i th Maxwell element in the assemblage is composed of a spring of rigidity $G_{\infty i}$ in series with a dashpot of viscosity η_{oi}, where G_∞ and η_o have the same meaning as before.

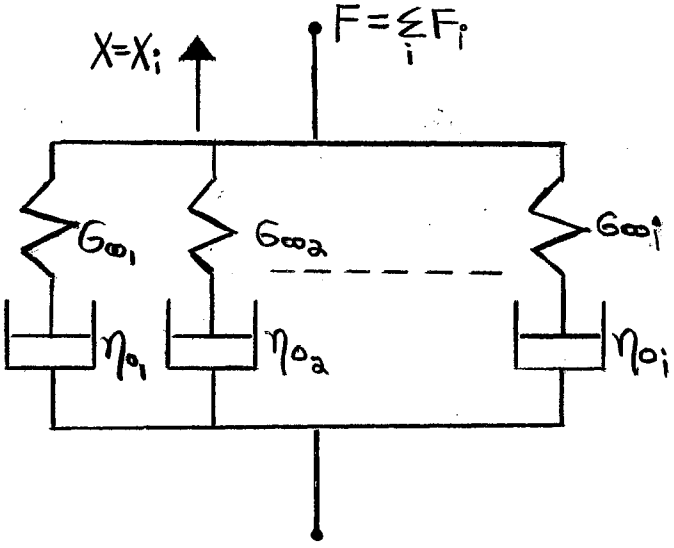

Figure 8. The parallel assemblage of Maxwell elements representing a unit volume of complex test fluid; F is analagous to the shearing stress, T, acting on the unit volume if test fluid, and X is analagous to the strain, e, undergone by the unit cube of test fluid.

The force F acting on the unit cube is the sum of the forces acting on the i Maxwell elements. The extension of the material is common to all the i Maxwell elements.

Equations (3.13), (3.14), (3.15) and (3.18) and the impedance analog justify describing the parameters of the parallel array by

$$\eta' = \sum_i \frac{G_{\infty i} J_i}{1+J_i^2 \omega^2} \tag{3.19}$$

$$\eta'' = \sum_i \frac{G_{\infty i} \omega J_i^2}{1+J_i^2 \omega^2} \tag{3.20}$$

$$G' = \omega \eta'' = \sum_i \frac{G_{\infty i} \omega^2 J_i^2}{1+\omega^2 J_i^2} \tag{3.21}$$

$$\eta = \sum_i \frac{G_{\infty i} J_i}{(1+\omega^2 J^2)^{1/2}} \tag{3.22}$$

$$\eta_s = \sum_i G_{\infty i} J_i \,. \tag{3.23}$$

The Maxwell specification of fluids will not yield resonance dispersion[25] of the complex shear viscosity. If a mass is placed in series with the spring and dashpot, the model will exhibit a resonance--force minimum for constant velocity. Inclusion of a mass in the model accompanies a consideration of inertial forces[25] on the microscopic scale. If frequencies are below several thousand cycles per second the inertial effects are small for most substances,[25,26] since the masses of the particles being displaced are small and the accelerations are small.

If there is only one relaxation mechanism--only one Maxwell element in the analagous model-- equations (3.19) and (3.20) take the

form

$$\eta' = \frac{G_{\infty_1}\mathcal{J}_1}{1+(\omega\mathcal{J}_1)^2} = \frac{G_{\infty_1}(\eta_{o_1}/G_{\infty_1})}{1+(\omega\mathcal{J}_1)^2} = \frac{\eta_{o_1}}{1+(\omega\mathcal{J}_1)^2} \tag{3.24}$$

$$\eta'' = \frac{G_{\infty_1}\omega\mathcal{J}_1^2}{1+(\omega\mathcal{J}_1)^2} = \frac{G_{\infty_1}(\omega\mathcal{J}_1)(\eta_{o_1}/G_{\infty_1})}{1+(\omega\mathcal{J}_1)^2} = \frac{\eta_{o_1}(\omega\mathcal{J}_1)}{1+(\omega\mathcal{J}_1)^2}. \tag{3.25}$$

The curves of η'/η_{o_1} and η''/η_{o_1} versus $\omega\mathcal{J}_1$ are displayed in figure 9.

C. Temperature Variation

If the temperature is changed from a reference Kelvin temperature T_o to a Kelvin temperature T, and if we assume that all the Maxwell elements in the parallel array specifying the fluid are affected in the same way, then the change in the η_{o_i} and G_{∞_i} can be described by

$$\eta_{o_i} = [F_1(T)][\eta_{o_i}^{\circ}] \tag{3.26}$$

$$G_{\infty_i} = [F_2(T)][G_{\infty_i}^{\circ}], \tag{3.27}$$

where F_1 and F_2 are functions of T, and $\eta_{o_i}^{\circ}$ and $G_{\infty_i}^{\circ}$ are the values of η_{o_i} and G_{∞_i} at the reference temperature. If equation (3.26) is divided by equation (3.27) the result is

$$\frac{\eta_{o_i}}{G_{\infty_i}} = \frac{F_1}{F_2}\frac{\eta_{o_i}^{\circ}}{G_{\infty_i}^{\circ}}, \tag{3.28}$$

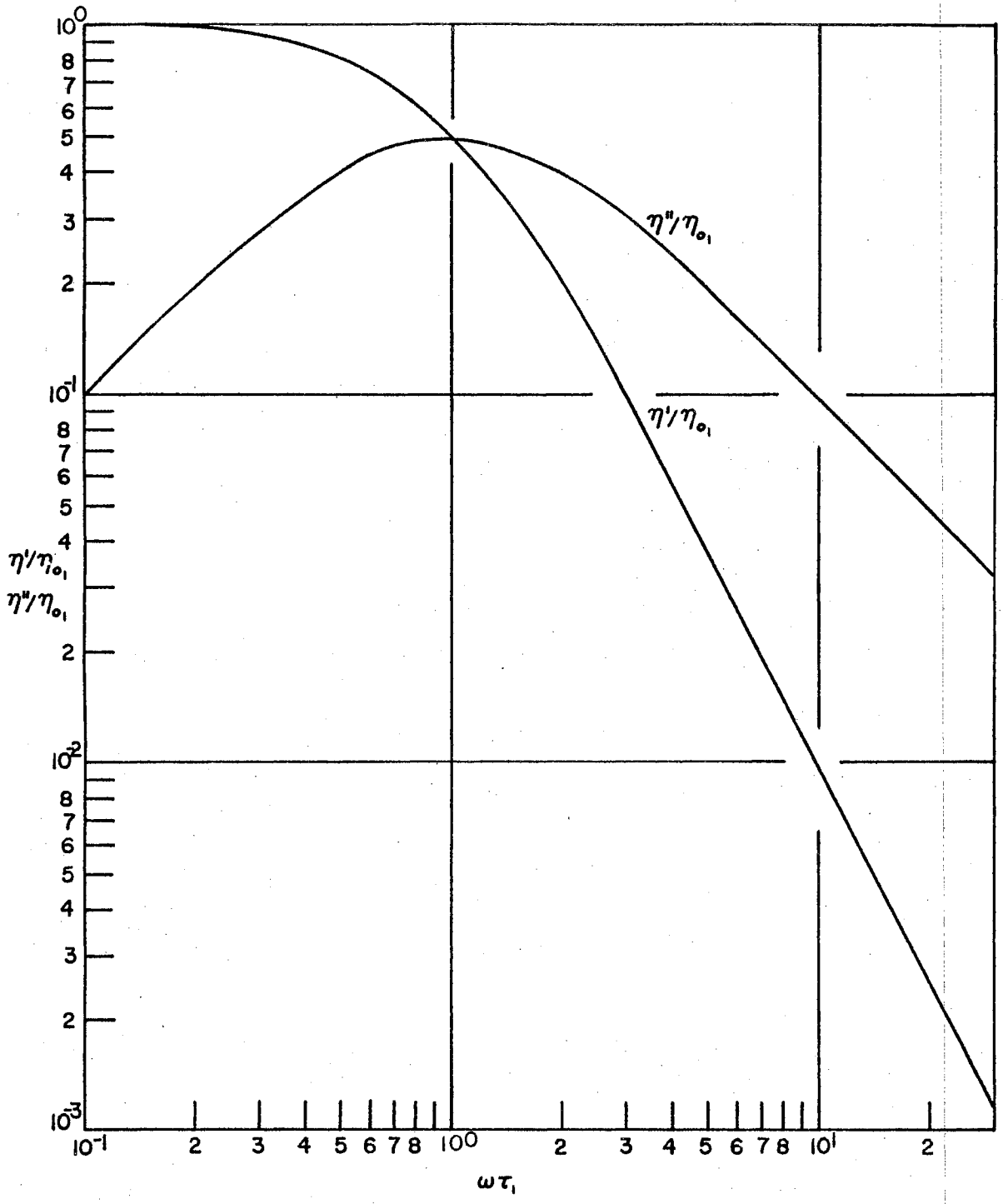

Figure 9. The theoretical normalized real and imaginary components of the complex dynamical viscosity versus normalized frequency for a single Maxwell element of relaxation time τ_1 with a dashpot of viscosity η_{o_1}.

or

$$\tau_i = \frac{F_1}{F_2}\,\tau_i^\circ = a_T\,\tau_i^\circ, \tag{3.29}$$

where τ_i is the relaxation time of the i th Maxwell element at temperature T, τ_i° is the relaxation time of the ith Maxwell element at temperature T_o, and a_T is a function of T.

When equations (3.27) and (3.29) are incorporated in equations (3.19), (3.20) and (3.23) the result is

$$\eta' = \sum_i \frac{F_2 G_{\infty i}^\circ (F_1/F_2)\,\tau_i^\circ}{1+[(F_1/F_2)\,\omega\,\tau_i^\circ]^2} = F_1\,\eta^{\circ\prime} \tag{3.30}$$

$$\eta'' = \sum_i \frac{F_2 G_{\infty i}^\circ\, \omega[(F_1/F_2)\,\tau_i^\circ]^2}{1+[(F_1/F_2)\,\omega\,\tau_i^\circ]^2} = F_1\,\eta^{\circ\prime\prime} \tag{3.31}$$

$$\eta_s = \sum_i F_2 G_{\infty i}^\circ (F_1/F_2)\,\tau_i^\circ = F_1\,\eta_s^\circ, \tag{3.32}$$

where η_s°, $\eta^{\circ\prime}$ and $\eta^{\circ\prime\prime}$ are the values of η_s, η' and η'' at T_o; η' and η'' are functions of ω, and $\eta^{\circ\prime}$ and $\eta^{\circ\prime\prime}$ are functions of a reduced frequency-- $\omega F_1/F_2$.

Equations (3.30) and (3.31) demonstrate that dynamical data at different temperatures should superpose if η'/F_1 and η''/F_1 are plotted against $\omega F_1/F_2$, since such a plot transforms η' and η'' at any temperature T and frequency ω into the reference $\eta^{\circ\prime}$ and η_o'' at frequency $\omega F_1/F_2$.

Equations (3.30), (3.31) and (3.32) may be solved for F_1 yielding

$$F_1 = \eta'/\eta_0' \tag{3.33}$$

$$F_1 = \eta''/\eta_0'' \tag{3.34}$$

$$F_1 = \eta_s/\eta_s^0 . \tag{3.35}$$

Equation (3.35) indicates that F_1 can be obtained from the ratios of the steady flow viscosities (η' for $\omega\lambda \ll 1$) at the two temperatures. Equations (3.33) and (3.34) indicate that F_1 can be obtained from the ratio of the imaginary components of the dynamical viscosities at the two temperatures and the ratio of the real components of the dynamical viscosities at the two temperatures; since η_0' is the value of η' at temperature T_0 and at a frequency F_1/F_2 times the frequency for the corresponding η' at temperature T , F_2 must be specified at least as a function of F_1 . Further, successive approximation will be necessary in equation (3.33) and (3.34) in order to obtain F_1 from dynamic data. If F_2 is not to be written as a function of F_1 , F_1 may be obtained from steady flow measurements, and then F_2 may be obtained from equations (3.33) and (3.34) by successive approximations utilizing F_1 .

If the functions F_1 and F_2 have been determined, and thus a_T in equation (3.29) is known, a plot of log a_T against temperature provides a convenient comparison point with theory and past measurements. Empirical studies[17] have revealed that, when the reduction of variables is successful for many different polymers, a_T could be

represented by

$$\log a_T = -C_1^\circ (T - T_0)/(C_2^\circ + T - T_0), \qquad (3.36)$$

where T_0 is an arbitrary reference Kelvin temperature, T is the test Kelvin temperature, and C_1° and C_2° are constants to be determined empirically.

Statistical mechanical, thermodynamical, and hydrodynamical theories yield a_T,[17] and can provide values for the constants in equation (3.36). Thus, if a valid theory is available, empirical determination of the constants in equation (3.36) allow the determination of the statistical mechanical quantities--position distribution functions, free volume and molecular mobility--, thermodynamic quantities--thermal expansion coefficients and activation energies--, and hydrodynamical quantities--solvent viscosity and friction coefficients.

Williams, Landel and Ferry[14] demonstrate a particular application of the functions describing the change in relaxation times. They found that a_T, after a suitable choice of reference Kelvin temperature T_s, can be expressed by

$$\log a_T = -8.86 (T - T_s)/(10.6 + T - T_s). \qquad (3.37)$$

Over a T range of $T_s \pm 50^\circ$ Kelvin, equation (3.37) applies to a wide variety of polymers, polymer solutions, organic glass-forming liquids, and inorganic glasses. T_s is usually chosen to lie about 50 degrees above the glass transition temperature. Williams, Landel,

and Ferry[14] obtain, from a_T data, information concerning the increase in the thermal expansion coefficient at the glass transition temperature, the fractional free volume at that point, and the dependence of free volume on temperature.

Fletcher and Gent[15] present reduced variable curves and curves of a_T versus T for some rubber-like materials and demonstrate how to obtain values of the dynamical shear properties at temperatures other than measurement temperatures from graphical presentations at standard temperatures.

Ferry, Fitzgerald, Grandine, and Williams[16] present reduced variable curves and a curve of a_T versus T for some polymers of high molecular weight. They obtain a check of experimental results by obtaining a distribution function of relaxation times by calculation from dynamical data.

D. Concentration Variation

If the concentration is changed from a reference concentration C_0 to a concentration C, and if we assume that all the Maxwell elements in the parallel array specifying the fluid are affected in the same way, then the change in the η_{0_i} and G_{∞_i} can be described by

$$\eta_{0_i} = F_3 \eta_{0_i}^{\circ} \tag{3.38}$$

$$G_{\infty_i} = F_4 G_{\infty_i}^{\circ}, \tag{3.39}$$

where F_3 and F_4 are functions of C, and $\eta_{0_i}^{\circ}$ and $G_{\infty_i}^{\circ}$ are the values of η_{0_i} and G_{∞_i} at the reference concentration. If

equation (3.38) is divided by equation (3.39) the result is

$$\frac{\eta_{oi}}{G_{\infty i}} = \frac{F_3}{F_4}\frac{\eta_{oi}^{\circ}}{G_{\infty i}^{\circ}}, \tag{3.40}$$

or

$$\lambda_i = \frac{F_3}{F_4}\lambda_i^{\circ} = a_c \lambda_i^{\circ}, \tag{3.41}$$

where λ_i is the relaxation time of the i th Maxwell element at concentration c, λ_i° is the relaxation time of the i th Maxwell element at concentration c_o, and a_c is a function of c.

When equations (3.39) and (3.41) are incorporated in equations (3.19), (3.20) and (3.23) the result is

$$\eta' = F_3 \eta^{\circ\prime} \tag{3.42}$$

$$\eta'' = F_3 \eta^{\circ\prime\prime} \tag{3.43}$$

$$\eta_s = F_3 \eta_s^{\circ}, \tag{3.44}$$

where η_s°, $\eta^{\circ\prime}$ and $\eta^{\circ\prime\prime}$ are the values of η_s, η' and η'' at c_o; η' and η'' are functions of ω, and $\eta^{\circ\prime}$ and $\eta^{\circ\prime\prime}$ are functions of a reduced frequency-- $\omega F_3/F_4$.

The reduction of data and determination of the functions F_3 and F_4 are identical to the same processes for the case of temperature variation presented previously.

E. Temperature and Concentration Variation

The equations applicable to varying concentration and temperature

may be obtained by multiplying coefficients in equations (3.30) and (3.42) and in equations (3.31) and (3.43). The results are

$$\eta' = F_1 F_3 \eta^{o\prime} \tag{3.45}$$

$$\eta'' = F_1 F_3 \eta^{o\prime\prime}, \tag{3.46}$$

where the superscript "o" now refers to the reference concentration at the reference temperature; η' and η'' are functions of ω, and $\eta^{o\prime}$ and $\eta^{o\prime\prime}$ are functions of a reduced frequency-- $\omega \frac{F_1 F_3}{F_2 F_4}$.

Equations (3.45) and (3.46) indicate that data at different temperatures and concentrations should superpose if η'/F_1F_3 and η''/F_1F_3 are plotted against $\omega \frac{F_1F_3}{F_2F_4}$, since such a plot transforms η' and η'' at any concentration C, temperature T and frequency ω into the reference $\eta^{o\prime}$ and $\eta^{o\prime\prime}$ at frequency $\omega \frac{F_1F_3}{F_2F_4}$, concentration C_o and temperature T_o.

F. Use of Reduced Parameters in Predicting the Mechanical Properties of a Fluid

Prediction of η' and η'' from $\eta^{o\prime}$ and $\eta^{o\prime\prime}$ is just the opposite procedure from that for reduction of all η' and η''. Then equations (3.45) and (3.46) demonstrate that one may obtain η' and η'' versus frequency at some concentration C and temperature T from measurements of $\eta^{o\prime}$ and $\eta^{o\prime\prime}$ at C_o and T_o by shifting the $\eta^{o\prime}$, $\eta^{o\prime\prime}$ versus frequency curves so that the frequency scale becomes $\omega \frac{F_2F_4}{F_1F_3}$ and the $\eta^{o\prime}$, $\eta^{o\prime\prime}$ scales become $F_1F_3\eta^{o\prime}$ and $F_1F_3\eta^{o\prime\prime}$.

G. Application of Reduced Parameters and Analagous Models to Specific Fluid Structures

Ferry[1] obtained a successful reduction of dynamical mechanical parameters of concentrated polymer solutions by assuming that all relaxation times of the Maxwell elements in the parallel array representing the fluids were multiplied by the same constant, a_T, when the temperature was changed from a reference temperature T_o to the test temperature T; he assumed that all relaxation times were multiplied by the same constant, a_c, when the concentration was changed from a reference concentration C_o to the test concentration C. Then a_T and a_c are the quantities which appear in equations (3.29) and (3.41), since those equations were derived from the assumption that all the Maxwell elements in the parallel array specifying the fluid are affected in the same way when the temperature and concentration are varied.

Ferry[1] assumed that the rigidity mechanisms of high polymers are rubber-like, so that the rigidities of the springs of the Maxwell elements in the parallel array specifying the fluid vary directly as the temperature; then F_2 in equation (3.27) is T/T_o, and equation (3.29) indicates that F_1 is $\frac{T}{T_o} a_T$ when T/T_o is substituted for F_2.

Ferry[1] found that the measured dynamical properties of concentrated polymer solutions could be described by reduced parameters only if he assumed that the rigidities of the springs of the Maxwell elements in the parallel array specifying the fluid vary directly as the concentration; in that case F_4 in equation (3.39) is C/C_o, and equation (3.41) indicates that F_3 is $\frac{C}{C_o} a_c$.

Riseman and Kirkwood[27] predicted the viscoelastic behavior of dilute solutions of rod-like and coiled macromolecules. They assumed that the

random motions of a particle can be described by a distribution function which gives the probability that the particle at a given time will be located at a specified position with a specified velocity. They took into account the disorienting effect of Brownian motions, which previous theories of viscosity[28] had failed to do. They assumed that the influence of the surroundings on the particle can be split into two separate components, one systematic, and the other characteristic of the fluctuating Brownian motions. They assumed that equilibrium is described by setting the hydrodynamic torques equal to the rotary diffusional torques. It turns out that the current density is made up of a diffusive part and a convective part, where the solvent motion contributes to the convective part.

Riseman and Kirkwood[27] assumed that the presence of a polymer molecule in a flowing fluid perturbs the flow because of the resistance offered by each monomer unit, so that a point in the fluid distant from the molecule will suffer a change in flow which is the sum of the perturbations of each of the monomeric units, and the effects present at one monomeric unit would contribute to the effects at any other monomeric unit. They assumed that the friction coefficient is the same for all monomeric units of the coil or rod, and that the value of the friction coefficient depends both on the fluid and the structure of the monomer. They assumed that the monomers were connected by a bond of fixed distance and angle. They assumed that the individual macromolecules do not interact, so that the energy dissipation and storage due to n molecules is n times that for one molecule.

Rouse[29] points out that the theory of the linear viscoelastic properties of dilute solutions of coiling molecules is inapplicable where there

are very rapid relaxation processes involving segments shorter than the monomer, or where segments of the coil are obstructed by other segments with which it happens to be in contact. He also points out that the polydispersity of any actual polymer would lead to error.

The viscous and elastic--energy storage--responses of a dilute solution will be determined by the interaction of the Brownian forces with the imposed forces, since those two forces provide the orienting and restoring forces which enhance the viscosity and establish the elasticity.[27] Experimental determinations of the frequency, concentration, and temperature variations of the dissipative and storage moduli of aqueous solutions of milling yellow dye--ranging from dilute to concentrated -- are available in chapter IV for examination for the presence of the behavior predicted below by examination of the varying role of the Brownian forces.

If the driving frequency is continuously lowered while the amplitude of the displacement is held constant, and thus the rate of shear is lowered and the imposed forces become smaller, a frequency will be reached for dilute solutions where complete Brownian motion is approached,[26] the particles are completely disoriented[26], and further decreases in frequency cannot further affect the orientation; Frish and Simha[26] and Ferry[30] expect that under such conditions--where the particles are not significantly oriented by the imposed forces--the elastic effects will decline and the viscosity effects will vary slowly with further decreases of the imposed force.

If the driving frequency is continuously raised while the amplitude of the displacement is held constant, a frequency will be reached for dilute solutions where the imposed forces become large and where there is no time for reorientations of the suspended particles during a period of

alternation[30]; again Frish's and Simha's[26] and Ferry's[30] interpretation of particle orientations requires that the elastic effects decline and the viscosity effects vary slowly with further frequency increases.

If the frequency of drive and the amplitude of the displacement are held constant as the temperature of a dilute solution is raised, a temperature will be reached where the Brownian forces are large compared to the imposed force, the particles are completely disoriented, and increases in temperature cannot further affect particle orientation; Frish's and Simha's[26] and Ferry's[30] interpretation of particle orientations then requires that the elastic effects decline and the viscosity effects vary slowly with further temperature increases.

At low temperatures the effect of the Brownian forces declines and complete particle orientation is approached; Frish's and Simha's[26] and Ferry's[30] interpretation of particle motions then requires that the elastic effects decline and the viscosity effects vary slowly with further temperature decreases (assuming that there is no structure build-up at low temperatures).

For low concentrations the viscous and elastic effects will approach those of the solvent, since the limiting zero concentration is identical to the solvent. Frish and Simha[26] point out that as the concentration is increased from zero concentration the particles at first do not interact, and the viscous and elastic effects are established by the sum of the effects of the individual particles. They state that as the concentration is increased, the contributions of the individual particles are no longer independent, the interactions at first being divisible into 2, 3, etc., particle interactions. As the concentration continues to increase, the viscous and elastic effects may vary in a complicated way, since the

hydrodynamic interactions become complex. Frish and Simha[26] expect that at the concentration at which close packing sets in, a strong and abrupt increase in the viscosity of the suspension occurs; presumably the magnitude of the elastic effects would change abruptly also, since the forces which enhance the viscosity are the forces which establish the elasticity.[27] They point out that at higher concentrations complicated structures--such as networks--may be established which impede the flow seriously. The disorienting effects of the Brownian motions will then be small, and the dissipative and restoring forces will be generated by molecular bonding.[30] As the available space decreases with increasing concentration--approaching sedimentation--the viscous and elastic effects will vary slowly since the motion of the solvent becomes severly impeded and only the molecular bonds--which respond only at high frequencies[29]--can contribute to the viscosity and elasticity as the concentration is increased.[30]

Ferry[1] presented the mechanical models corresponding to Reisman's and Kirkwood's theoretical viscoelastic behavior of dilute rigid rods and flexible coils and described experimental verification of the theories. The models are shown in figure 10. An unlimited number of Maxwell elements are required in the parallel assemblage describing the viscoelastic behavior of coils. $\eta_{o\ solution}$ is the steady state value of the viscosity of the solution. The values of the other quantities in the model were given by Ferry[31] in terms of the steady state viscosity of the solvent, $\eta_{o\ solvent}$, and are given for rods by

$$G_{\infty_1} = 3CRT/5M \tag{3.47}$$

$$\eta_{op} = (\eta_{o\ solution} - \eta_{o\ solvent})/4 \tag{3.48}$$

$$\eta_{o_1} = 3(\eta_{o\ solution} - \eta_{o\ solvent})/4, \tag{3.49}$$

where R is the gas constant, M is the molecular weight of the rod, C is the concentration in grams per cubic centimeter, and T is the Kelvin temperature. The values for coils are given by

$$G_{\infty_1} = CRT/M \tag{3.50}$$

$$\eta_{o_1} = 6(\eta_{o\,\text{solution}} - \eta_{o\,\text{solvent}})/\pi^2, \tag{3.51}$$

where M is the molecular weight of the coils. Ferry[31] points out that the values for rigid ellipsoids are quite similar to those for rods, and gives references to enforce his statement.

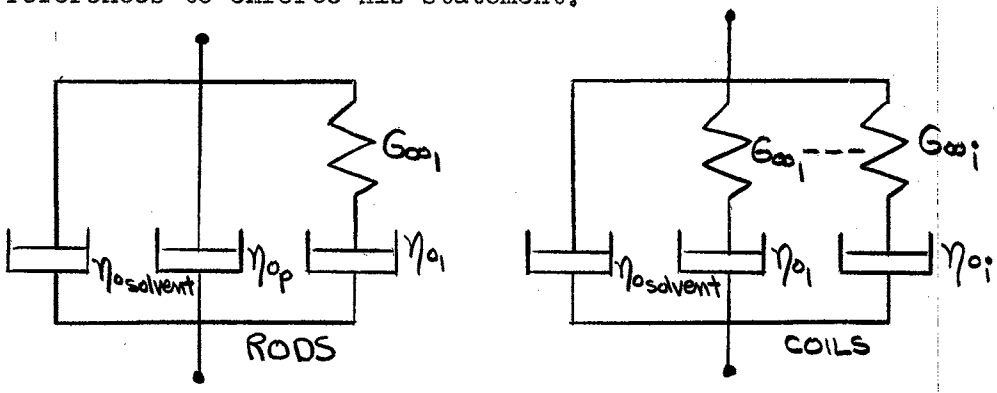

Figure 10. Mechanical models corresponding to the theoretical viscoelastic behavior of dilute rigid rods and flexible coils.

Dividing equation (3.49) by equation (3.47) yields

$$J_1 = \frac{\eta_{o_1}}{G_{\infty_1}} = \frac{5M}{4CRT}(\eta_{o\,\text{solution}} - \eta_{o\,\text{solvent}}). \tag{3.52}$$

Taking the ratio of J_1 at temperature T and concentration C to J_1° at temperature T_o and concentration C_o from equation (3.52) yields

$$\frac{J_1}{J_1^\circ} = \frac{\eta_{o\,\text{solution}} - \eta_{o\,\text{solvent}}}{\eta_o^\circ\,\text{solution} - \eta_o^\circ\,\text{solvent}} \frac{C_o T_o}{CT} \frac{M}{M_o}, \tag{3.53}$$

and taking the ratio of G_{∞_1} at temperature T and concentration C to $G_{\infty_1}^\circ$ at temperature T_o and concentration C_o from equation (3.47) yields

$$\frac{G_{\infty_1}}{G_{\infty_1}^{\circ}} = \frac{C T}{C_0 T_0} \frac{M_0}{M} \qquad (3.54)$$

Equation (3.52) demonstrates that a distribution of molecular weights will result in a distribution of relaxation times for solutions of rigid rods. Equations (3.53) and (3.54) demonstrate that if the molecular weight associated with each relaxation mechanism does not change when the temperature and concentration change, then all relaxation times are multiplied by the same function of temperature and concentration, and the G_∞ vary directly as the temperature and concentration. Manipulation of equations (3.50) and (3.51) lead to the same conclusions concernign solutions of coils. The conclusions are applicable to solutions of rigid ellipsoids, since the forms of the equations for the values of the quantities in the analagous model are the same for rods and ellipsoids.[31] Thus, Ferry's[1] previously described assumptions concerning the concentration and temperature dependence of the rigidity mechanisms and the relaxation times of the Maxwell elements representing high polymer solutions are applicable to dilute solutions of rods, ellipsoids or coils, providing that the rods, ellipsoids, and coils do not change their molecular weight with changing concentration and temperature.

Figure 11 displays η'/η_{0_1} and η''/η_{0_1} versus $\omega\vartheta_1$ curves yielded by the model analagous to rods shown in figure 10, and figure 12 displays η'/η_{0_1} and η''/η_{0_1} versus $\omega\vartheta_1$ curves yielded by the model analagous to coils shown in figure 10. The curves for rods were obtained by writing out equation (3.19) and (3.20) for the specific rod model; those equations then become

$$\eta' = \eta_{0\,\text{solvent}} + \eta_{0p} + \frac{\eta_{0_1}}{1+(\omega\vartheta_1)^2} \qquad (3.55)$$

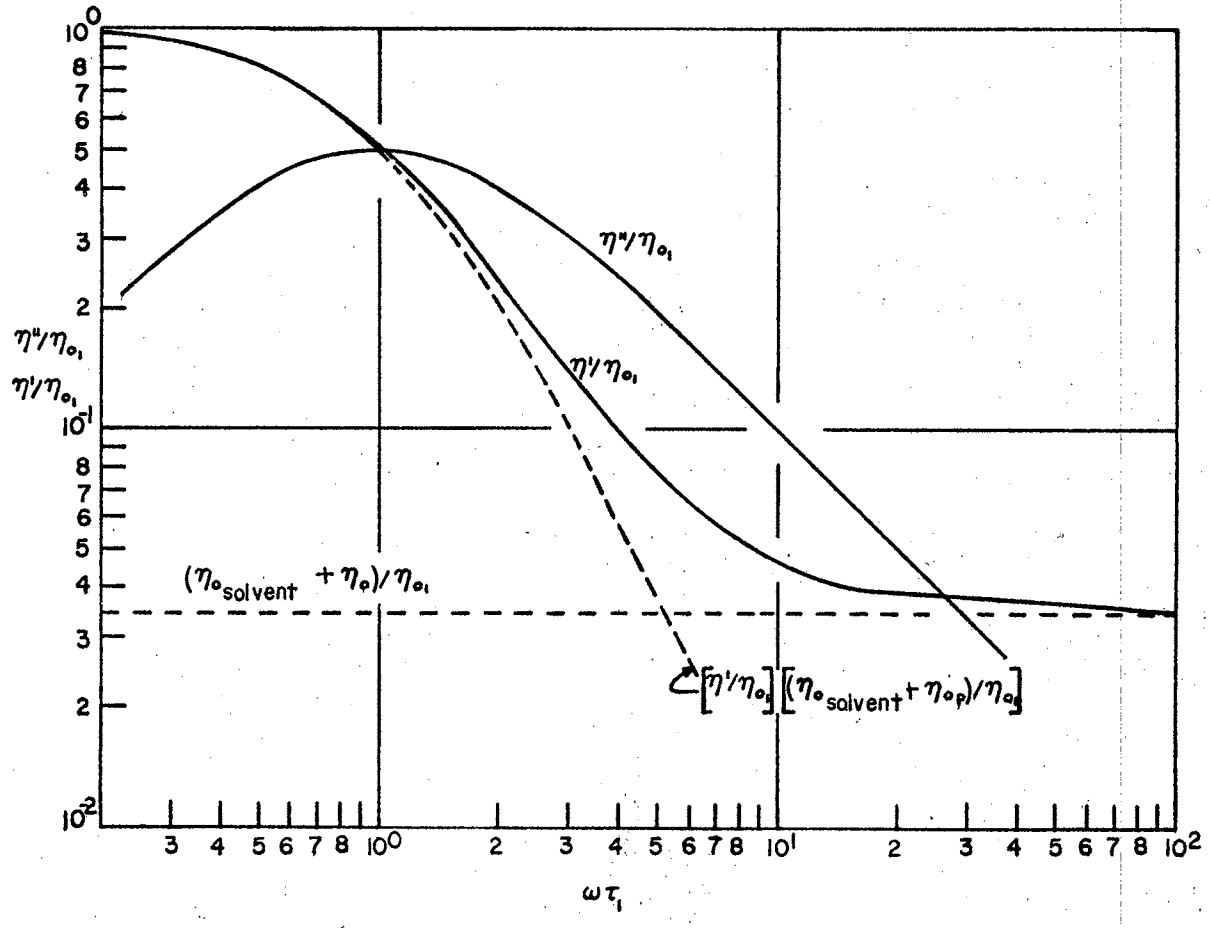

Figure 11. The normalized real and imaginary components of the complex dynamical viscosity versus normalized frequency, as predicted by the statistical mechanical theory for independent rod-like particles.

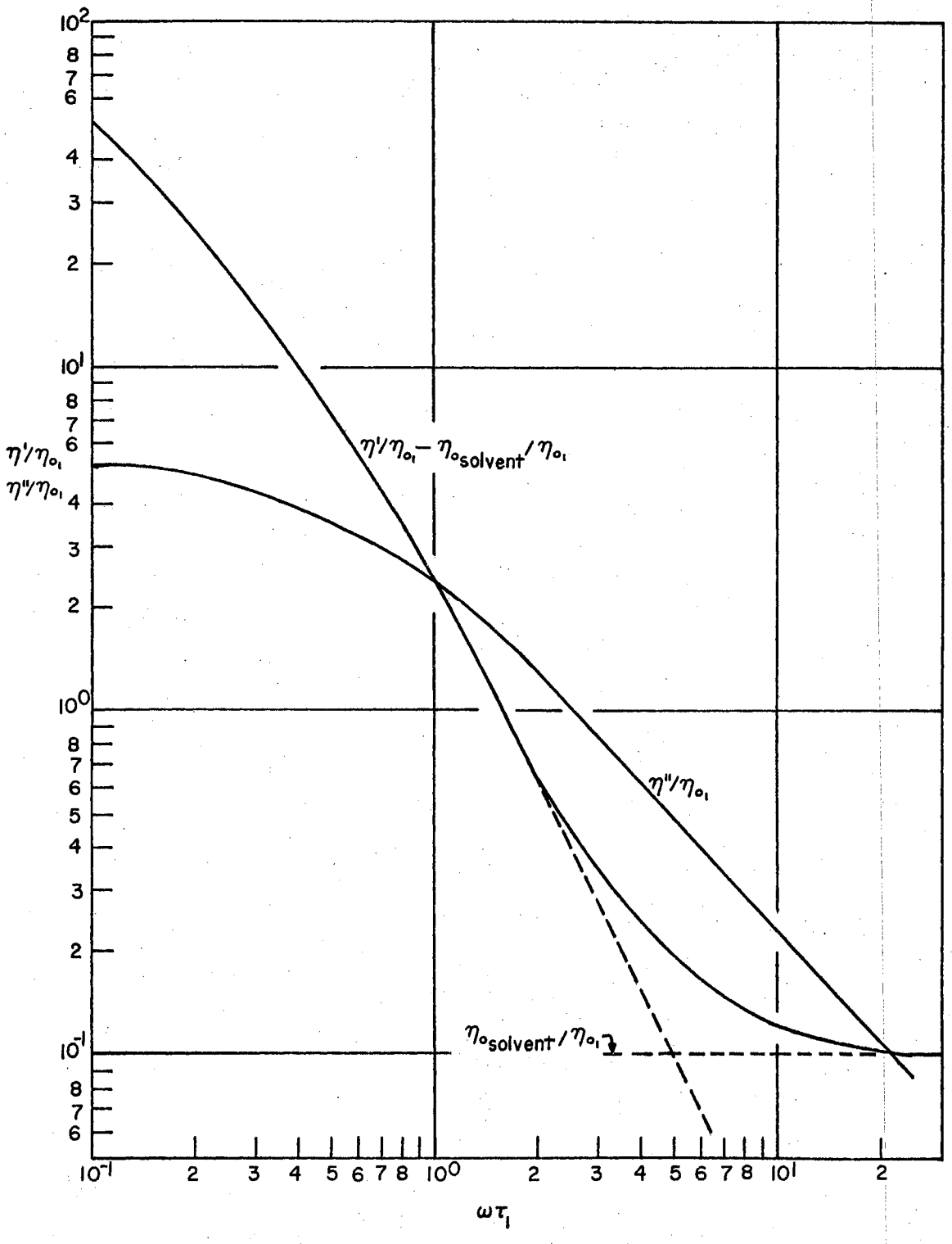

Figure 12. The normalized real and imaginary components of the complex dynamical viscosity versus normalized frequency, as predicted by the statistical mechanical theory for independent coils.

$$\eta'' = \frac{\eta_{o_1}}{1+(\omega\lambda_1)^2} . \tag{3.56}$$

Dividing both sides of equations (3.55) and (3.56) and transposing the term independent of $\omega\lambda_1$ in equation (3.55) the result is

$$\left[\frac{\eta'}{\eta_{o_1}}\right] - \left[\frac{\eta_{o\,\text{solvent}} - \eta_{o_p}}{\eta_{o_1}}\right] = \frac{1}{1+(\omega\lambda_1)^2} \tag{3.57}$$

$$\frac{\eta''}{\eta_{o_1}} = \frac{\omega\lambda_1}{1+(\omega\lambda_1)^2} . \tag{3.58}$$

In order to obtain the curves in figure 12 it was necessary to assume a relationship among the η_{o_i} and G_{∞_i} in the model analagous to coils shown in figure 10. The assumptions were that

$$\eta_{o_i} = i\eta_{o_1}, \; i = 1,2,3\ldots, \tag{3.59}$$

and the G_{∞_i} are equal and constant. These assumptions reduce to the assumption that there are equal numbers per unit volume of chains which are 1, 2, 3,...n times the length of a reference chain of minimum length; assuming that there are lengths intermediate to these changes the results little, as will be explained later. The curves in figure 12 were obtained by incorporating the assumptions relating the η_{o_i} and the G_{∞_i} in equations (3.19) and (3.20) for the specific coil model; those equations then became

$$\eta' = \eta_{o\,\text{solvent}} + \sum_i \frac{i\eta_{o_i}}{1+(i\omega\lambda_1)^2} \tag{3.60}$$

$$\eta'' = \sum_i \frac{i\eta_{o_1}(i\omega\lambda_1)}{1+(i\omega\lambda_1)^2} . \tag{3.61}$$

Dividing both sides of equation (3.60) and (3.61) and transposing the term independent of $\omega\lambda_1$ in equation (3.60) the result is

$$\frac{\eta'}{\eta_{0_1}} - \frac{\eta_{0\,solvent}}{\eta_{0_1}} = \sum_i \frac{i}{1+(i\omega\lambda_1)^2} \qquad (3.62)$$

$$\frac{\eta''}{\eta_{0_1}} = \sum_i \frac{i^2(\omega\lambda_1)}{1+(i\omega\lambda_1)^2}. \qquad (3.63)$$

The summations were continued until the last term calculated changed the sum of terms by less than 10%. If the η_{0_1}, and thus the chain lengths, are assumed to change more slowly than the change described by equation (3.59), the number of terms required for less than 10% change of the sum is about the same, and the sum is about the same.

It would be more accurate to assume a continuous distribution of lengths and go to an integral form for η' and η''. However, a more significant correction would be to introduce a known distribution of number of particles per unit volume versus particle length.

The theory upon which the models are based yields a limiting value for η' for high frequencies which is independent of distributions of particle length, so that comparison with experiment may be accomplished for that limiting case if the low frequency limit of η' for the solution and solvent is known.

CHAPTER IV

EXPERIMENTAL RESULTS

A. The Variation of η^* with Frequency

Figure 13 displays the real and imaginary components of the complex dynamical viscosity coefficient versus frequency for a 1.70% aqueous milling yellow solution at 21.5 degrees centigrade to 21.75 degrees centigrade; the 150 cycles per second point is connected by a dotted portion of the curve because the measurement temperature was 21.3 degrees centigrade--.2 degrees lower than the preceeding points--, which means that η' may not level off as sharply as the curve would indicate.

The tube samples used in obtaining figure 13 ranged from 5 tubes 2.695 centimeters long and .192 centimeter in diameter at 2 cycles per second to 32 tubes 1.169 centimeters long and .0394 centimeter in diameter at 200 cycles per second.

B. The Variation of η^* with Concentration

Figure 14 displays the real and imaginary components of the complex dynamical viscosity coefficient versus concentration for aqueous milling yellow solutions at 24 degrees centigrade and driving frequency of 25 cycles per second. The fluids were obtained from a 1.95% base solution by dilution with distilled water. The base solution was diluted with the proper amount of water to give the desired concentration, and the diluted solutions were then brought to the boiling point, after

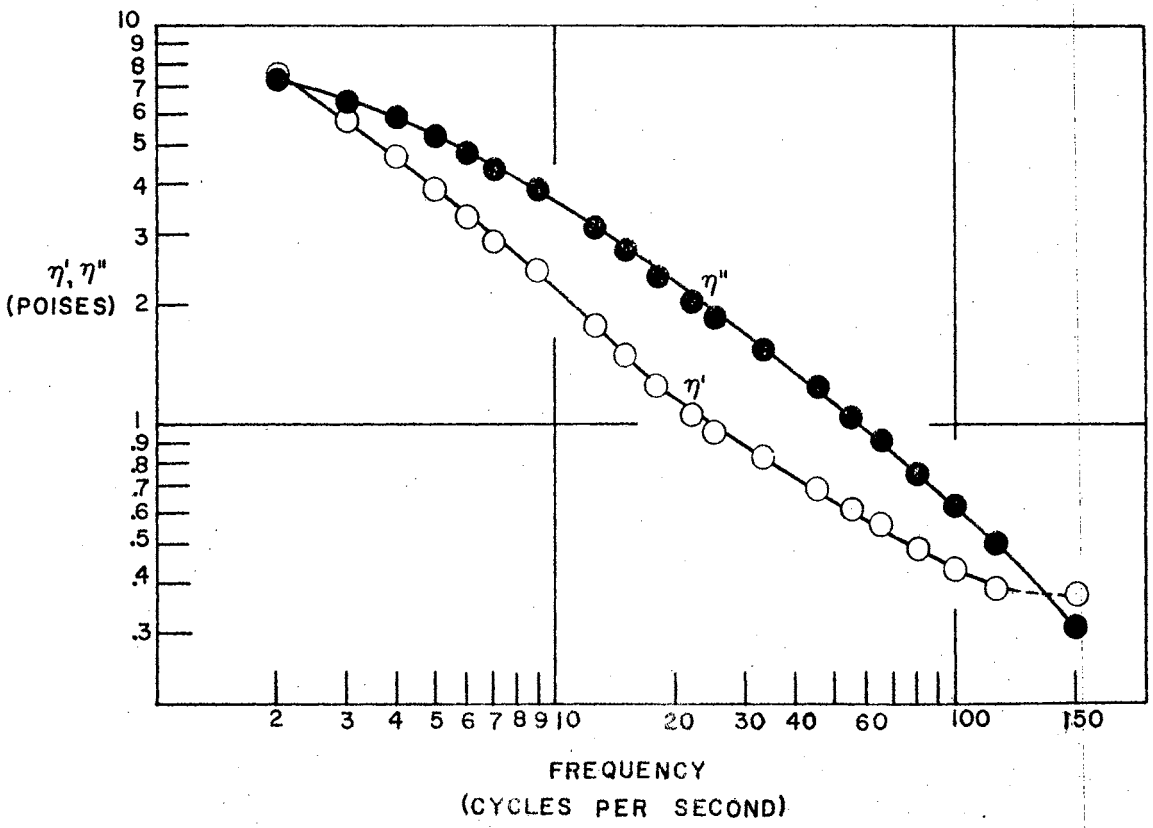

Figure 13. The real and imaginary components of the complex dynamical viscosity versus frequency, for a 1.70% aqueous milling yellow solution.

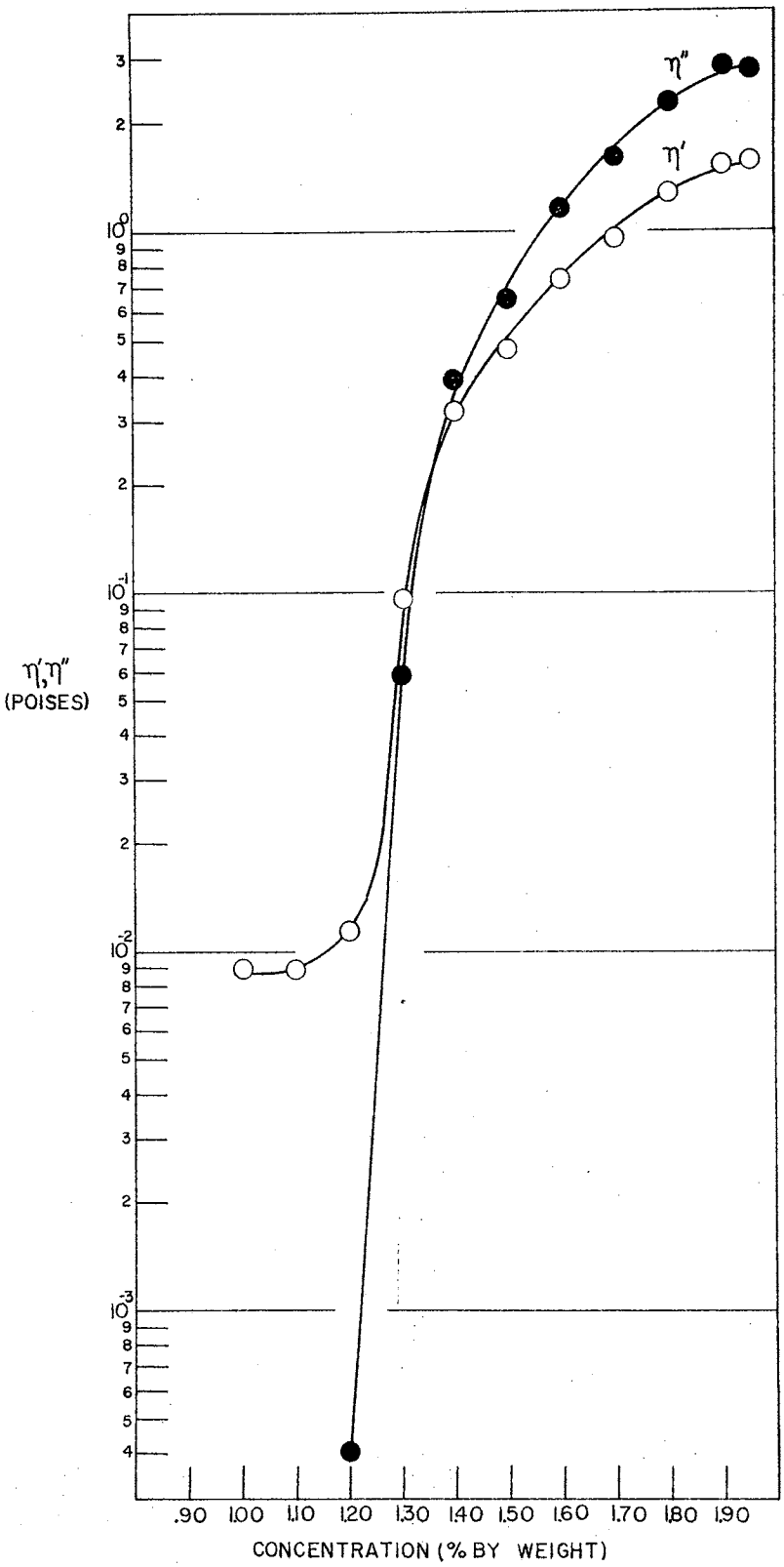

Figure 14. The real and imaginary components of the complex dynamical viscosity versus concentration, for aqueous milling yellow solutions at 24 degrees centigrade and 25 cycles per second.

which they were allowed to return to room temperature. All of the soltuions were heated in the same water bath for the same time so that their relative concentrations would remain accurate, although their absolute concentrations might deviate slightly from the calculated values. A very sharp decrease in η' and η'' is noted for concentrations approaching 1.20%, and below 1.20% no measurements of η'' can be made because inertial effects predominate.

The limiting value of η' at low concentration agrees well with the handbook value for the steady flow viscosity of water at 24 degrees centigrade.

The tube samples used in obtaining figure 14 ranged from 55 tubes .7950 centimeter long and .0333 centimeter in diameter at 1.00% to 23 tubes 1.639 centimeters long and .106 centimeter in diameter at 1.95%.

C. The Variation of η^* with Temperature

Figure 15 displays the real and imaginary components of the complex dynamical viscosity coefficient versus temperature for a 1.70% aqueous milling yellow solution at 25 cycles per second. A very sharp decrease in η' and η'' is noted for temperature approaching 45 degrees centigrade, and above 45 degrees centigrade no measurements of η'' can be made because inertial effects predominate. The limiting value of η' at high temperatures differs from the handbook value for the steady state viscosity of water at those temperatures by 18%, but is still decreasing with increasing temperature so that η' tends to level off at a value equal to the steady state viscosity of water at high temperatures.

The decrease in η' and η'' below 10 degrees centigrade is probably

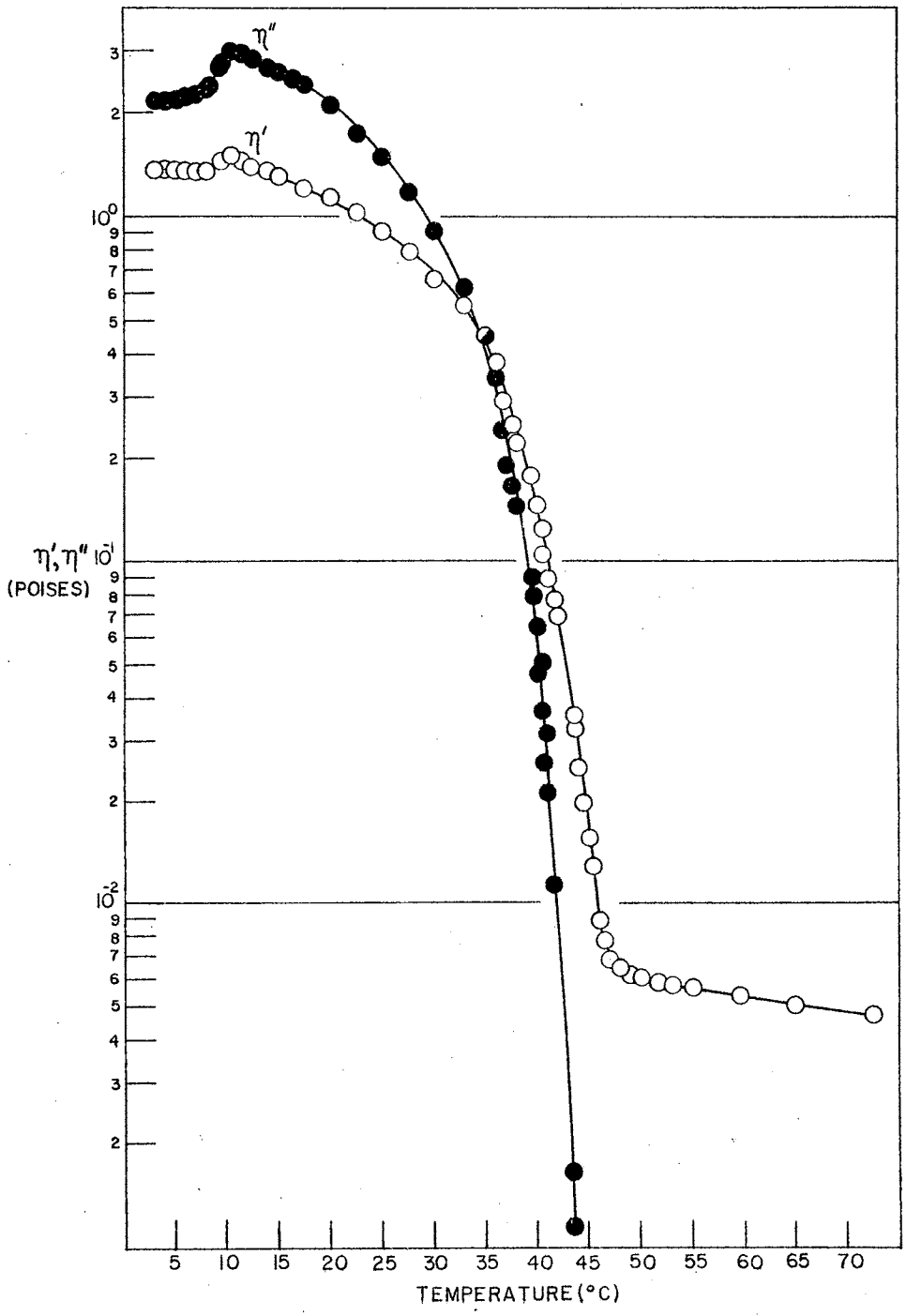

Figure 15. The real and imaginary components of the complex dynamical viscosity versus temperature, for a 1.70% aqueous milling yellow solution at 25 cycles per second.

due to changes in fluid structure, since the fluid becomes cloudy and finely divided milling yellow solids appear in the fluid below 5 degrees centigrade--one might suspect that the process begins at a microscopic level before it is visually observable.

The tube samples used in obtaining figure 15 ranged from 23 tubes 1.639 centimeters long and .106 centimeter in diameter at 5 degrees centigrade to 55 tubes .7950 centimeter long and .0333 centimeter in diameter at 70 degrees centigrade.

D. The Reduced Parameters

An attempt was made to apply Ferry's[1] previously described assumptions concerning the concentration and temperature dependence of the rigidity mechanisms and the relaxation times of the Maxwell elements representing high polymer solutions to the experimental data. Chapter III included a demonstration that Ferry's reduction of parameters should also be valid for dilute solutions of rods, ellipsoids and coils, providing that the rods, ellipsoids, and coils do not change their molecular weight with changing temperature and concentration.

When Ferry's choices of F_1 and F_2, described in section G of chapter III, were substituted into equations (3.26) and (3.27), and when the successive approximations were carried out in equations (3.33) and (3.34), non-converging series were obtained for F_1 (and for F_3— obtained from similar equations for concentration variation). It was possible to obtain converging series by empirical choices of the relationship between F_1 and F_2 and between F_3 and F_4, but the choices require improbable interpretations of microscopic mechanisms if the fluid is assumed to be composed of rods, ellipsoids, or chains.

For example, if one assumes that the viscosity mechanism involves independent contributions of the individual particles while the rigidity mechanism involves two particle interaction, the rigidities of the Maxwell elements specifying the fluid might be taken to vary as the square of the change in the viscosities of the Maxwell elements; such an assumption yields converging series for the factors by which all relaxation times are multiplied when the temperature and concentration are changed, and places the reduced parameters in range.

The curves shown in figure 11 for the theoretical η^* versus ωD_1 were assigned experimentally measureable values by calculating a molecular weight obtained by assuming that the particles were of the average size indicated by the electron microscope, dividing by the length of a monomer estimated from the molecular diagram to get the number of monomers, and multiplying by the molecular weight of a monomer to get the molecular weight of a particle. η_0 solution was taken to be the low frequency value of η'. The resulting curve yielded poor agreement with experiment. It would have been necessary to choose a low frequency vlaue of η' inconsistent with the theoretical curve in order to force better agreement. Altering the assumed size of the particles in order to force better agreement for high frequencies would have lessened agreement at low frequencies. The curves would have been little different if rigid ellipsoids had been assumed, since the values of the rigidities and viscosities of the Maxwell elements of the model describing ellipsoids are quite similar to those for rods.[31]

An attempt was made to empirically match the experimental η^* versus frequency curve to the curves displayed in figure 11; no match was possible which yielded a value of the limiting value of η'/η_0,

consistent with the theory which yielded the curves. Again it would have been necessary to choose a low frequency value of η' inconsistent with the theoretical curve in order to force better agreement of the high frequency value of η' with the predicted limiting value. This might cause one to wonder if the limiting high frequency was actually reached in the experiment described. However, comparison of the experimental and theoretical intersecting points of η' and η'' demands that the highest experimental frequencies reached be considered to fall in the limiting region.

As was explained in chapter III, section G, the high frequency limit of η' is independent of assumptions concerning length and concentration distribution of coils of different lengths. In order to make a comparison of η' for high frequency with the curve in figure 12, η_0 solution was taken to be the low frequency value of η'. The low frequency value of η' would have to decrease in order to have better agreement; but a decrease in η' with low frequency is inconsistent with theory, so the disagreement holds.

CHAPTER V

DISCUSSIONS OF EXPERIMENTAL RESULTS AND SUGGESTIONS FOR FURTHER STUDY

A. Discussion of Experimental Results

The general behavior of the experimental curve agrees well with the general behavior expected by analyzing the role of the Brownian motions as was done in chapter III, section G. For example, in figure 13 the vanishing of η'' at high temperature and the leveling off of η' toward a constant value agrees well with the concept that complete disorientation is obtained at high temperature. The fact that the limit of η' is near the high temperature values of the viscosity of water implies that even the friction interactions between solvent and suspended particles are small, which could be due to the decrease in the viscosity of the solvent, change in particle size, or both. The sudden increase of η' and η'' near 1.20% in figure 14 agrees well with Frish's and Simha's[26] expectation mentioned in chapter III, section G, that at the concentration at which close packing sets in, a strong and abrupt increase in the viscosity of the suspension occurs and with the argument described later which indicates that the particles should begin to overlap within the range of concentrations covered by the presented measurements.

The failure of the reduced parameter theory to yield a reduction of data at all temperatures and concentrations implies, from the

arguments of chapter III, that if the fluid is composed of rods, ellipsoids, or coils or some combination of rods, ellipsoids, and coils, then the basic particles are changing their molecular weight with changing temperature and concentration, or the basic particles interact, or both. But Ferry[1] successfully applied the reduced parameter theory where strong interaction was known to occur; then it must be the changing molecular weight which prevents application of the reduced parameter theory.

The failure of the model representing the statistical mechanical theory to yield the proper frequency variation of η' and η'' at a single temperature and concentration implies, from the arguments of chapter III, that if the fluid is composed of rods, ellipsoids or coils, then there is a distribution of molecular weights at a given temperature and concentration as Prados and Peebles[11] indicate, or the basic particles interact, or both.

Since the assumptions concerning particle length do not account for the deviation from rod and chain theory for the high frequency limit of η', it must be that the assumption concerning independence of individual particle contributions has been contridicted. Thus if chains or rods are responsible for the viscoelastic behavior of the milling yellow solutions, then they interact at 1.70% concentration near room temperature.

Perhaps some infinite array of Maxwell elements could be constructed empirically which would yield the proper η^* versus frequency curve, but the frequency range obtained in this study is not sufficient to justify such an effort; further, the model would be difficult to interpret without further knowledge of the structure of the fluid.

Ferry[1] expresses doubt as to whether a single reduction function could be employed for all the relaxation mechanisms for extremely dilute solutions where he expects the solvent viscosity to enter explicitly. The η^* versus concentration curve for milling yellow demonstrates that the solvent viscosity enters explicitly near a concentration of 1.20%, since at concentrations below 1.20% η' rapidly approaches the steady state viscosity of water and η'' becomes immeasureable.

Further evidence of the significance of hydrodynamic forces in the range of 1.20% can be obtained from measurements by Prados and Peebles[11]; they assumed that milling yellow particles are rod-shaped, and developed a diffusion constant based on that assumption which they utilized to calculate particle sizes from extinction angle measurements of aqueous milling yellow solutions in a concentration range included in this study. The particle shapes and sizes obtained by Prados and Peebles[11] agree well with electron microphotographs of "raw" milling yellow powders mentioned in chapter II, section D.

Calculations based on the assumption of the correctness of the particle sizes given by Prados and Peebles[11] and the electron microscope--assuming a density of 1 gram per cubic centimeter for the pure polymer--indicate that for concentrations in the range of 1.20% the milling yellow particles have a volume available to them whose cube root is very near 2 particle lengths, so that the particles have about 1 particle length clearance between them. It seems plausible, then, that in the concentration range of 1.20% the particles cease to overlap, friction between particles declines in importance, and the hydrodynamic forces met by the individual particles would begin to predominate.

As mentioned earlier, one might expect the overlap of particles to occur where the abrupt and strong change in η' and η'' occurs--near 1.20%.

There may be error generated in Prados' and Peebles' method[11] by assuming that the particles do not interact with each other. There may also be error generated in the calculation of overlap concentration by assuming that the particle sizes are the same for the solution concentration used by Prados and Peebles (1.36%) and for a 1.20% solution; there is also certainly an error proportional to the error in assuming the density of milling yellow to be 1 gram per cubic centimeter.

It was previously stated that the particles must change their length with changing concentration; yet the lengths indicated by the electron microscope--where the concentration of the fluid being examined was changed greatly from the test concentration--agree with Prados' and Peebles' determination of particle size for the test concentrations. These two seemingly contradictory facts can be caused to be consistant if one considers the possibility that the particle lengths do not change with concentration for quasi-equilibrium concentration changes such as those involved in preparing a sample for the electron microscope--where the fluid evaporates at room temperature--, while the particle lengths do change with concentration for the disturbing preparation procedure for the test fluids--where the fluids were heated and quickly cooled.

B. Conclusions

It appears that the test system and mathematical relations examined in this study are adequate for obtaining the complex dynamical viscosity

of fluids in the range of 10^{-3} to 10 poises as a function of temperature and concentration from 2 to 200 cycles per second.

The reduced parameter theory based on analagous models failed severely when applied to the measured dynamical parameters of the milling yellow solutions. However, the failure of the theory indicates directions for further research.

There is enough evidence for the existence of rigid ellipsoidal particles in the milling yellow solutions to justify a continued consideration of such particles; however, if such particles are responsible for the viscoelastic behavior of the solutions, then there is a distribution of sizes of particles which changes in a complex way with changing temperature and concentration, and the suspended elements overlap at most concentrations of interest.

Visual observations of aging milling yellow solutions have revealed many complex structures: crystals, chains, networks, star-shaped clusters, and leaf-shaped clusters. One should, then, consider possible contributions of all of these structures and more in constructing, applying and interpreting a reduced parameter theory for milling yellow solutions.

C. Suggestions for Further Study

The measurements described in this study should be extended to lower frequencies by altering the methods of examining the pressure, displacement and velocity monitor outputs; the measurements could be extended to higher frequency or lower rigidities by providing tube samples with many small tubes, providing sample flexure does not become significant. An extended frequency range would justify a concentrated

attempt to construct a particular analagous model which would yield the curves obtained from experiment. Low frequency measurements (near .01 cycles per second) would provide further use of reduced parameter method by bringing the equations derived for $\omega\tau \ll 1$ into the range of applicability.

If the suspended milling yellow particles could be caused to be uniform in size at some fixed temperature and frequency, perhaps by filtering or by ultrasonic agitation,[10] better agreement with theory might be obtained. Once agreement with theory was obtained for constant temperature and concentration it whould be possible to determine the way in which the particle sizes change with temperature and concentration.

Milling yellow solutions prepared from various solvents could be subjected to alternating magnetic or electric fields, and the dynamical mechanical properties measured while varying the frequency of mechanical drive or while varying the frequency of electric or magnetic drive. Such measurements should provide not only information concerning the structure of the fluids and the relation among the macroscopic electric and magnetic properties, but should also provide information concerning the structure of the individual particles.

Measurements of the complex dielectric coefficient as a function of the frequency of electric drive at a fixed frequency of mechanical drive or at fixed frequency of electrical drive and varying frequency of mechanical drive would provide further information relating mechanical and electrical properties; even more significant is the fact that such measurements would aid the formation of a stress-optic law.

Attempts should be made to further determine the size and shape of the milling yellow particles in aqueous solutions. Such attempts would involve independent measurements of optical scattering--to get the size, shape and radial distribution of particles--, of mobility of foreign substances--to get the size of particle aggregates--, and of filtering rates--to get particle sizes. An observation of the optical transmission of the milling yellow powders suspended in distilled water and in an inert fluid would yield information concerning possible chemical changes induced by the water. X-ray scattering would provide an indication of the state of the milling yellow powders.

The milling yellow solutions should be subjected to shear rates which force them into non-linear regions--where the real and imaginary components of the complex dynamical viscosity coefficient are a function of shear rate--to possibly gain information concerning the degree of particle alignment and interaction[32] and the strength of the Brownian forces.[33]

The higher concentration milling yellow solutions should be examined for the presence of thixotropy[34]--reversible structure changes--by attempting to establish a hysteresis loop[34] of the real and imaginary components of the complex dynamical viscosity coefficient versus increasing and decreasing shear rate at fixed temperature, frequency and concentration. The hysterisis loop would give some information concerning the strength of particle interactions compared with the strength of the Brownian actions.[34]

LIST OF REFERENCES

1. J. D. Ferry, "Mechanical Properties of Substances of High Molecular Weight. VI Dispersion in Concentrated Polymer Solutions and its Dependence on Temperature and Concentration," J. Am. Chem. Soc., 72, 3746 (1950).

2. G. B. Thurston, "Theory of Oscillation of a Viscoelastic Fluid in a Circular Tube," J. Acoust. Soc. Am., 32, 210 (1960).

3. G. B. Thurston, "Measurement of the Acoustic Impedance of a Viscoelastic Fluid in a Circular Tube," J. Acoust. Soc. Am., 32, 1091 (1961).

4. G. B. Thurston, "Apparatus for Absolute Measurement of Analagous Impedance of Acoustic Elements," J. Acoust. Soc. Am., 24, 649 (1952).

5. F. R. Eirich, "Introduction to Rheological Concepts," from Rheology, edited by F. R. Eirich, Academic Press, Inc., New York, Volume I, Chapter 1 (1956).

6. M. Reiner, "Phenomenological Macrorheology," from Rheology, edited by F. R. Eirich, Academic Press, Inc., New York, Volume I, Chapter 2 (1956).

7. G. B. Thurston and J. K. Wood, "End Corrections for a Concentric Circular Orifice in a Circular Tube," J. Acoust. Soc. Am., 25, 861 (1953).

8. Van Nostrand's Scientific Encyclopedia, Third Edition, D. Van Nostrand Company, Inc., Princeton, New Jersey, page 546 (1958).

9. Alastair W. Hunter, Chief Chemist, National Aniline Division, Suite 430, Merchandise Mart Plaza, Chicago 54, Illinois.

10. H. Freundlich and C. W. Gillings, "The Influence of Ultrasonic Waves on the Viscosity of Colloidal Solutions," Trans. Faraday Soc., 34, 649 (1938).

11. J. W. Prados and F. N. Peebles, "A Study of Laminar Flow Phenomena Utilizing a Doubly Refracting Liquid," Progress Report 2, "Determination of the Flow Double Refraction Properties of Aqueous Milling Yellow Dye Solutions," Published Master's Thesis under Contract No. Nonr-811(04), Knoxville, Tennessee, Engineering Experiment Station and Department of Chemical Engineering of the University of Tennessee (1955).

12. E. H. Honeycutt, Jr. and F. N. Peebles, "A Study of Laminar Flow Phenomena Utilizing a Doubly Refracting Liquid," Progress Report 3, "Rheological Properties of Aqueous Solutions of Milling Yellow Dye," Published Master's Thesis under Contract No. nonr-811(04), Knoxville, Tennessee, Engineering Experiment Station and Department of Chemical Engineering of the University of Tennessee (1955).

13. J. D. Ferry, W. M. Sawyer and J. M. Ashworth, "Behavior of Concentrated Polymer Solutions Under Periodic Stresses," J. Polymer Science, 2, 593 (1947).

14. M. L. Williams, R. F. Landel and J. D. Ferry, "The Temperature Dependence of Relaxation Mechanisms in Amorphous Polymers and Other Glass-forming Liquids," J. Am. Chem. Soc., 77, 3701 (1955).

15. W. P. Fletcher and A. N. Gent, "Dynamic Shear Properties of some Rubber-like Materials," British J. App. Physics, 8, 194 (1957).

16. J. D. Ferry, E. R. Fitzgerald, L. D. Grandine, Jr. and Malcom L. Williams, "Temperature Dependence of Dynamic Properties of Elastomers; Relaxation Distributions," Ind. and Eng. Chem., 44, 703 (1952).

17. J. D. Ferry, Viscoelastic Properties of Polymers, John Wiley and Sons, Inc., New York, Chapter 11 (1961).

18. J. M. Burgers, First Report on Viscosity and Plasticity, Noord-Hollandsche, Amsterdam (1935).

19. T. Alfrey and P. Doty, "The Methods of Specifying the Properties of Viscoelastic Materials," J. App. Physics, 16, 700 (1945).

20. Turner Alfrey, Jr. and E. F. Gurnee, "Dynamics of Viscoelastic Behavior," from Rheology, edited by F. R. Eirich, Academic Press, Inc., New York, Volume I, Chapter 11 (1956).

21. F. R. Eirich, "Brief Survey of Weissenberg's General Theory of Deformation, and of the Basic Relations of Sinusoidal Deformations," from Rheology, edited by F. R. Eirich, Academic Press, Inc., New York, Volume I, Appendix to Introduction to Rheological Concepts (1956).

22. A. Gemant, "The Conception of a Complex Viscosity and its Application to Dielectrics," Trans. Faraday Soc. 31, 1582 (1935).

23. R. B. Lindsay, Mechanical Radiation, The Maple Press Company, York, Pa. for McGraw-Hill Book Company, Inc., Chapter 9 (1960).

24. A. J. Barlow and J. Lamb "The Visco-elastic Behavior of Lubricating Oils Under Cyclic Shearing Stress," Proc. Roy. Soc. (London), 253, 52 (1959).

25. Edwin R. Fitzgerald, "Mechanical Resonance Dispersion in Metals at Audio-Frequencies," Phys. Rev., 108, 690 (1957).

26. H. L. Frisch and Robert Simha, "The Viscosity of Colloidal Suspensions and Macromolecular Solutions," from Rheology, edited by F. R. Eirich, Academic Press, Inc., New York, Volume I, Chapter 14 (1956).

27. J. Riseman and J. G. Kirkwood, "The Statistical Mechanical Theory of Irreversible Processes in Solutions of Macromolecules," from Rheology, edited by F. R. Eirich, Academic Press, Inc., New York, Volume I, Chapter 13 (1956).

28. J. G. Kirkwood, "Viscoelastic Properties of Macromolecules," Rec. trav. chim. 68, 649 (1949).

29. P. E. Rouse, "A Theory of the Linear Viscoelastic Properties of Dilute Solutions of Coiling Polymers," J. Chem. Phys. 21, 1272 (1953).

30. J. D. Ferry, Viscoelastic Properties of Polymers, John Wiley and Sons, Inc., New York, Chapter 10 (1961).

31. J. D. Ferry, "Rheology of Macromolecular Systems," Rev. Mod. Phys., 31, 130 (1959).

32. A. Gemant, "Structural Viscosity," from Frictional Phenomena, Chemical Publishing Co., Inc., New York, Chapter IX (1950).

33. I. M. Krieger and T. J. Dougherty, "A Mechanism for Non-Newtonian Flow in Suspensions of Rigid Spheres," Trans. Soc. Rheol., III, 137 (1959).

34. H. Green, "Thixotropy," from Industrial Rheology and Rheological Structures, Wiley and Sons, Inc., New York, Chapter 4, (1949).

VITA

Richard Allen Ely

Candidate for the Degree of

Master of Science

Thesis: MEASUREMENT AND REDUCTION OF DYNAMICAL MECHANICAL PARAMETERS OF AQUEOUS SOLUTIONS OF MILLING YELLOW DYE

Major Field: Physics

Biographical:

Personal Data: Born in Ponca City, Oklahoma, June 27, 1936, the son of Lucille and John Ely.

Education: Attended grade school in Ponca City, Oklahoma; was graduated from Ponca City Senior High School in Ponca City, Oklahoma, in 1954; was graduated from U. S. Naval School, Electronic Technician, Class "A," Service School, NTC, Great Lakes Illinois in 1955; received the Bachelor of Science degree from Oklahoma State University, with a major in Physics, May 1960; completed the requirements for the Master of Science degree in May, 1962.

Honors, Honorary Organizations, and Professional Organizations: Honorary Member, Ponca City Engineer's Club, 1954; Dean's Honor Roll, Oklahoma State University, spring 1957, fall 1957, spring 1958, fall 1958, spring 1959, fall 1959; Outstanding Graduating Senior in Physics, Oklahoma State University, 1960; Member, Phi Kappa Phi, National Honorary Scholastic Society; Member, Sigma Pi Sigma, National Honorary Physics Society; Associate Member, Acoustical Society of America.

Professional Experience: Maintaining electronic communicating devices, U. S. Naval Air Station, Hutchinson, Kansas, 1955; Research Assistant, Acoustics Laboratory, Oklahoma State University, Stillwater, Oklahoma, 1960, 1961, 1962.